Characterizing snow instability with avalanche problem types derived from snow cover simulations

Benjamin Reuter, Léo Viallon-Galinier, Simon Horton, Alec van Herwijnen, Stephanie Mayer, Pascal Hagenmuller, Samuel Morin

Cold Regions Science and Technology 194 (2022) 103462

Contents lists available at ScienceDirect

Cold Regions Science and Technology

journal homepage: www.elsevier.com/locate/coldregions

Characterizing snow instability with avalanche problem types derived from snow cover simulations

Benjamin Reuter [a,b,*], Léo Viallon-Galinier [a,c,d], Simon Horton [e], Alec van Herwijnen [b], Stephanie Mayer [b], Pascal Hagenmuller [a], Samuel Morin [a]

[a] Univ. Grenoble Alpes, Université de Toulouse, Météo-France, CNRS, CNRM, Centre d'Etudes de la Neige, 38000 Grenoble, France
[b] WSL Institute for Snow and Avalanche Research SLF, Davos, Switzerland
[c] UR ETNA, INRAE, Université de Grenoble Alpes, France
[d] École des Ponts, Champs-sur-Marne, France
[e] Simon Fraser University, Burnaby, Canada

A B S T R A C T

Snow cover models support avalanche forecasting. However, despite much development to derive snow instability from snow cover model output, snow cover models presently do not provide information on avalanche problem types – an essential element to describe avalanche danger. We present an approach to detect, track and assess weak layers in snow cover model output data and assess the related avalanche problem types. We classify different avalanche situations into new snow, wind slab, persistent weak layer and wet-snow problems for either natural or artificial avalanche release. We demonstrate the applicability of this approach with both SNOWPACK and Crocus model output for several winter seasons at Weissfluhjoch, Switzerland, and two sites in Western Canada. At Weissfluhjoch, simulation results from both models coincided reasonably well with avalanche activity recorded with a seismic avalanche detection system. Over a 16-year period both models produced similar frequencies of avalanche problems. At the two Canadian sites frequencies of simulated avalanche problem types agreed fairly well with the observed frequencies. The results provide confidence that avalanche problem types can be simulated in different snow climates and that changes due to climate change can be studied. Moreover, the approach to assess avalanche problem types holds potential to support operational avalanche forecasting.

1. Introduction

Many natural hazards are closely tied to local weather conditions. Both, past and current weather are important for forecasting snow avalanches (LaChapelle, 1966). Snow cover models simulate the evolution of the snow cover based on measured or simulated weather data over the course of a winter season (Morin et al., 2020). The models Crocus (Brun et al., 1992; Brun et al., 1989) within the SAFRAN–SURFEX/ISBA–Crocus–MEPRA model chain (Durand et al., 1999; Lafaysse et al., 2013; Vionnet et al., 2012) and SNOWPACK (Bartelt and Lehning, 2002; Lehning et al., 2002a; Lehning et al., 2002b) resolve snow stratigraphy which allows for assessing snow instability – the snowpack's propensity to avalanche.

As verifications with observations have shown, the models can reproduce distinct characteristics of the natural snow stratigraphy such as faceted crystals or melt-refreeze layers (Calonne et al., 2020) – even if they are driven with numerical weather prediction data (Bellaire and Jamieson, 2013; Durand et al., 1999). Also, weak layers showing poor stability in stability tests were represented in simulated stratigraphy (Monti et al., 2014). However, snow cover models are sensitive to meteorological input, and uncertainties can affect snow instability modelling (Richter et al., 2020) which depends on the simulated snow layering. Ensemble simulations (Vernay et al., 2015) allow to estimate the range of uncertainties. As snow cover models were initially designed to support avalanche forecasting, tools for snow instability assessment were implemented (Giraud et al., 2002; Schweizer et al., 2006). Advances in the understanding of slab avalanche release (Schweizer et al., 2016a) have led to improvements of snow instability indicators concerning the skier stability index (Monti et al., 2016), the critical crack length (Gaume et al., 2017) or the liquid water content index (Mitterer et al., 2013; Wever et al., 2016). Comparisons with avalanche data showed that dry-snow instability indicators for skier triggering (Reuter and Bellaire, 2018) and wet-snow instability forecasts (Bellaire et al., 2017) identify the major avalanche cycles but improvements are needed to decrease the rate of false alarms. For evaluation with field data, weak layers were either detected manually (Reuter et al., 2015b), or indices referred to the weakest layer (Schweizer et al., 2006) – and potentially switching between the weakest layers while the snowpack evolves.

* Corresponding author at: Univ. Grenoble Alpes, Université de Toulouse, Météo-France, CNRS, CNRM, Centre d'Etudes de la Neige, 38000 Grenoble, France.
E-mail address: reuter@slf.ch (B. Reuter).

https://doi.org/10.1016/j.coldregions.2021.103462
Received 25 May 2021; Received in revised form 26 November 2021; Accepted 7 December 2021
Available online 14 December 2021

Ideally, weak layers would be detected automatically and followed over the entire evaluation period to monitor their stability and how they contribute to the avalanche situation.

Characteristics of avalanche situations, such as spatial patterns or the temporal evolution of the instability, depend on weak layer type and slab properties (McClung and Schweizer, 1999). To explain the character of an avalanche situation in addition to the danger level, which mainly describes the degree of instability in a region (Techel et al., 2020), avalanche problem types were formulated in North America (Statham et al., 2018) and in Europe (EAWS, 2019). "New snow", "wind-drifted snow", "persistent weak layers", "wet-snow" or "gliding snow" are widely used by European avalanche forecasting services. North American forecasters use similar terms, but separate a "persistent" from a "deep-persistent slab avalanche problem type". Their classification also addresses "dry or wet loose snow avalanche problem types" or "cornice avalanche problem types". Avalanche problem types have – in both regions – phenomenological descriptions referring to typical stratigraphy and release mechanisms. The descriptions suit traditional avalanche forecasting practices when meteorological data are available, but snowpack information such as on the presence of a weak layer is often scarce. Snow cover modelling can provide this information and allows us to attempt automatic avalanche problem assessment. To this end, simulated stratigraphy, in particular weak layer type and slab properties, need to be interpreted in view of avalanche release and translated into avalanche problem types. Regarding weak layer type, non-persistent grain shapes have an initially weak microstructure (Bair, 2013), but soon become stronger due to equi-temperature metamorphism (Colbeck, 1998). On the other hand, faceted, depth hoar or surface hoar crystals, have extended life spans causing so called persistent avalanche problems (Jamieson and Johnston, 1995). For slab layer formation new snow and drifting snow are important drivers. The related avalanche problem types "new snow" and "wind slabs" often pose an acute avalanche problem for natural release and a short-lived avalanche problem in view of artificial triggering (de Quervain, 1966). Only in combination with a persistent weak layer, these short-lived avalanche problems remain susceptible to artificial triggering for more time. In the absence of new snow and drifting snow, wetting due to rain or snow melt may cause water to percolate down the snowpack (Baggi and Schweizer, 2009) leading almost exclusively to natural release (Schweizer et al., 2020). Following the avalanche release processes avalanche problem types (Fig. 1) can be derived based on simulated snowpack properties. This seems important for advancing numerical avalanche forecasting (Horton et al., 2020).

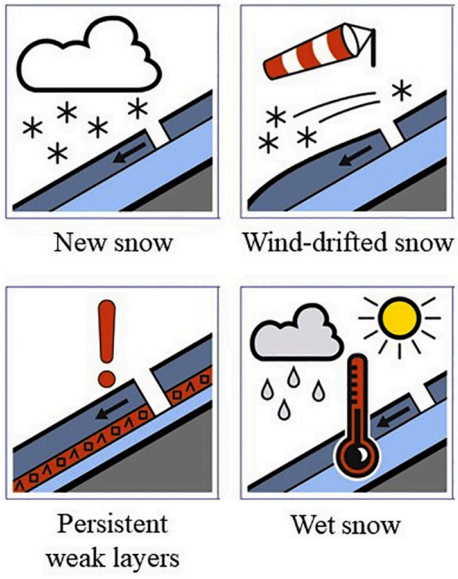

Fig. 1. Icons representing four major avalanche problem types used in Europe (EAWS, 2019).

Strength-over-stress criteria were suggested to describe natural dry-snow avalanche release (Roch, 1966), which is a consequence of a competition between the rate of loading from snowfall and the rate of strengthening in the buried weak layer (McClung, 1981). A simple concept along those lines was suggested (Conway and Wilbour, 1999) and only tested with non-persistent weak layers so far (Brown and Jamieson, 2008). Based on experiments with small snow samples Capelli et al. (2018) modeled the balance between healing of broken bonds and viscoelastic load redistribution among weak layer grains, which apparently drives the damage process leading to weak layer failure. This is partly considered by the parametrization of a strain rate dependent bond stress (Nadreau and Michel, 1986) used in the deformation rate stability index (Lehning et al., 2004), which has been evaluated to a limited extent (Nishimura et al., 2005). Developments regarding snow instability indicators focused on crack propagation (e.g. Gaume et al., 2017) – a process that is best observed in persistent weak layers. Evaluation with field observations was limited to indicators for artificial release and persistent weak layers (Birkeland et al., 2019; Richter et al., 2019).

With advances in snow cover modelling (Morin et al., 2020) simulated snow instability information can support avalanche forecasters by covering data sparse areas and filling temporal gaps. However, in practice avalanche forecasting still relies largely on experience-based weighing of indicators for snow instability and snow cover model output needs to be better aligned with the needs of avalanche forecasters. Avalanche problem types can provide a means to summarize simulated snow cover information for avalanche forecasters (Horton et al., 2019) and could be assessed automatically when simulated snow stratigraphy data are condensed into snow instability (Reuter and Bellaire, 2018). This requires progress in how snow cover models detect, track, and assess the stability of relevant weak layers and translate the corresponding information into avalanche problem types.

Predicting avalanche problem types from simulated snow cover data is worthwhile for avalanche forecasting and holds promise for improving climate change impact studies (Castebrunet et al., 2014). Being able to derive avalanche problem types from snow cover predictions for the next decades would allow us to better characterize future avalanche regimes. Here, we combine established knowledge on avalanche release processes and demonstrated suitability of snow instability indicators to derive avalanche problem types from snow cover model data. We present results obtained in different snow climates and compare the simulated avalanche problem types to avalanche observations and estimated avalanche problem types.

2. Data

We compiled meteorological, snow cover and avalanche data for Weissfluhjoch, Davos, Switzerland, Whistler, British Columbia (BC) and Rogers Pass in Glacier National Park, BC, Canada. The data sources we used include automatic weather stations, numerical weather forecasting models, manual observations and field measurements. With the meteorological input we ran SNOWPACK and Crocus simulations to obtain sets of snow stratigraphy for the three locations describing several seasons.

2.1. Study sites

We use data from the area around Davos, Eastern Swiss Alps including weather data measured at the automatic weather station at Weissfluhjoch, avalanche observations and snow profiles in the area around Weissfluhjoch, as well as seismic avalanche data measured at 2 sites less than 15 km from Weissfluhjoch. Moreover, for two sites in Western Canada, at Whistler, BC and Rogers Pass in Glacier National Park, BC we extracted meteorological data from forecasts of the GEM numerical weather prediction model. At the BC locations we used daily

estimates for avalanche problem types from local observers.

2.2. Meteorological data and snow cover simulations

For the simulations at Weissfluhjoch, we used meteorological measurements covering the winter seasons from 1999/2000 to 2015/2016 from an automatic weather station at the Weissfluhjoch study plot at an elevation of 2516 m in the Eastern Swiss Alps (Ménard et al., 2019; Wever, 2017). To run the snow cover model SNOWPACK we used the measured snow surface temperature (Dirichlet boundary conditions) and the measured snow height. We started simulations on 1 October, when no snow was present at the AWS. Crocus simulations (Vionnet et al., 2012) were driven with the same meteorological data set, but precipitation measurements rather than measured snow height were used. Simulations were initialized on 1 August using the settings described in Lafaysse et al. (2017). Mass and heat exchange with the atmosphere and soil were simulated with ISBA (Decharme et al., 2011) using Neumann boundary conditions. Events of drifting snow were estimated when the SNOWPACK variable "snow_transport_24_h" exceeded 0.4 kg/cm. For Crocus simulations, we estimated snow transport based on a threshold wind speed of 7.5 m/s (Li and Pomeroy, 1997). We did not utilize snow transport modules, but calculated a simple index which does not account for the feedback of snow transport on the snow cover (Lehning and Fierz, 2008). Both snow cover models, SNOWPACK and Crocus, ran until 31 May outputting snow profiles at 6:00 and 15:00 UTC.

For the simulations in Canada, we used numerical weather prediction model (NWP) data extracted from the 2.5 km version of the GEM model (Milbrandt et al., 2016) for the winter seasons from 2015/2016 to 2019/2020. We used data from two grid points, one close to Whistler, BC at 1917 m a.s.l. and one close to Rogers Pass in Glacier National Park, BC at 1863 m a.s.l.. SNOWPACK simulations were driven with precipitation amounts forecasted by the NWP model. The albedo and snow surface temperatures were simulated in SNOWPACK using Neumann boundary conditions with forecast values of incoming longwave and shortwave radiation. Wind speed forecasts over the period were irregular due to operational changes to the GEM model. As a result we do not show results for wind slab problems because the simulated snow transport variable was inconsistent. SNOWPACK was initialized depending on data availability at the latest on 15 September, when no snow was present and ran until 30 April, when local reference observations stopped for the season. Snow profiles were output at 6:00 and 15:00 local time.

The analysis described below requires the following snow cover properties to be extracted from the snow cover simulations: layer thickness, snow density, snow grain shape, shear strength and liquid water content for all simulated SNOWPACK and Crocus layers. Regarding meteorological output, the 24 h new snow, the snow depth as well as snow transport indicator or wind speed, are used from SNOWPACK and Crocus simulations, respectively.

2.3. Observation data

We use records of natural and triggered avalanches observed by the ski patrol at Weissfluhjoch to describe the avalanche situation from 26 December 2014 to 2 January 2015 along with snow profiles on slopes around Weissfluhjoch. Three snow profiles describe the situation when the avalanche activity peaked: a bi-monthly routine observation on 31 December at the Weissfluhjoch study plot, a field report on 31 December on a northwesterly aspect at Casannapass and a field report on 2 January at Wangegg on a northeasterly aspect. The snow profiles comply with common standards (Fierz et al., 2009; SLF, 2016) and contain compression or extended column test results (Jamieson, 1999; Simenhois and Birkeland, 2009). Repeated skier triggering or remote triggering of adjacent slopes prompted the two field reports. Although avalanche observations are available for most of the winter seasons, we selected this example because the field reports and personal observations allow associating observed avalanches to identified weak layers.

2.4. Forecast avalanche problem types

Avalanche problem types are issued at Whistler and Rogers Pass by public avalanche forecasting services based on a combination of local observations and assessments by local professionals according to North American standards (Statham et al., 2018). They include "dry loose", "wet loose", "storm slab", "wind slab", "persistent slab", "deep persistent slab" and "cornice" avalanche problems. To comply with European standards (EAWS, 2019) we neglected the avalanche problem types "dry loose", "wet loose" and "cornice". If a "storm slab" avalanche problem was reported for more than 3 consecutive days without snowfall or snow transport according to local observations, we changed the record after the 3 days to "no storm slab" avalanche problem, which occurred in 21% of the days in Whistler and on 32% of the days at Roger Pass. Natural release is limited to the snowfall period (Heck et al., 2019; Stoffel et al., 1998) and triggering typically becomes rare a few days after the storm (Bair, 2013; Gauthier et al., 2010). Observations include the seasons between 2015 and 2020 and are complete during 1 December to 30 April, except for 5 days at Whistler and 11 days at Rogers Pass.

2.5. Seismic avalanche data

Above Davos, two seismic arrays consisting of 7 seismic sensors (4.5 Hz vertical component geophones) were deployed during the winter-seasons between 2015 and 2018. Commercial data acquisition systems were used (Seismic Instruments Inc.) and data were continuously sampled at a rate of 500 Hz (for more details, see van Herwijnen and Schweizer (2011). The seismic arrays were deployed at the Wannengrat site (3 km from Weissfluhjoch) at an elevation of 2500 m a.s.l., and at the Dischma site (15 km from Weissfluhjoch) at an elevation of 2000 m a.s.l.. The detection range of these seismic arrays is typically around 3 km for larger avalanches (Heck et al., 2019).

To obtain an avalanche catalogue, we had at each site also installed several automatic cameras to provide ground truth data which allowed us to identify seismic signals generated by avalanches using the images. We processed these avalanche signals using a multichannel correlation analysis assuming planar wavefront propagation to identify coherent data within 5-seconds moving windows (Marchetti et al., 2020; Ulivieri et al., 2011). A similar approach is used to identify snow avalanches from other sources with infrasound array analysis, allowing for real-time monitoring and identification of snow avalanches at source-to-receiver distances of several kilometers (Marchetti et al., 2015; Mayer et al., 2020). Using the avalanche signals confirmed with the images from the automatic cameras, we then identified typical signal characteristics associated with avalanches. Specifically, for each site and each winter season, we defined threshold values for the minimum signal amplitude, minimum signal duration, maximum peak frequency content and maximum change in back azimuth. Using these threshold values, we then processed seismic data from the entire winter season to automatically identify signals potentially generated by avalanches. As the threshold values were rather lenient, in a last step, the automatically identified signals were visually inspected to remove falsely identified signals. While it is clear that visual inspection of seismic data is time consuming and prone to observer bias, given the overall similarities between the seismic signals generated by avalanches, we are quite confident in the accuracy of our visual inspection of the data. Avalanche occurrences from both sites were then pooled to create an avalanche catalogue for the region of Davos consisting of the release time of each avalanche found in the seismic data.

To evaluate conditions prone for natural release we use data from the winter season 2015–16. The data may be incomplete due to signal processing uncertainties or limited coverage with regard to a typical forecasting region which has several 100 km^2 such as the region of

Davos, even though the recording time is precise. Hence, the recorded avalanches are strong indicators for unstable conditions in the area. Non-observations, however, are a less strong indicators for stable conditions.

3. Methods

We introduce an algorithm to detect and track weak layers in SNOWPACK and Crocus snow cover simulations. The algorithm analyzes the following steps; simply, was a weak layer buried, is it relevant, is it unstable and how does it change with time? Based on the stability of the weak layers and the meteorological conditions we then assess avalanche problem types. For every day of the snow cover simulation, the algorithm identifies up to four avalanche problem types either in view of natural release or in view of artificial triggering.

3.1. Weak layer detection

The algorithm analyzes the simulated snow profiles every day at 6:00 and 15:00 local time. Running through the sequence of snow profiles and comparing each snow profile with the previous snow profile, the algorithm identifies the layers that were buried by snowfall. They are potential weak layers that need to be detected. The snow grain shape of the layers at or close to the surface prior to the snowfall allows us to distinguish two situations. We consider layers with persistent grain shapes that are located either at the snow surface or below a surface crust (Colbeck, 1991) prior to the snowfall as persistent weak layers. Layers with non-persistent grain shapes at the snow surface prior to the snowfall, or non-persistent grains depositing during a snowfall, are considered non-persistent weak layers (Fig. 2). The properties of buried potential weak layers, including current depth and grain shape, are then stored for tracking in later time steps.

We assess each weak layer's relevance for snow instability. We consider a weak layer relevant if a slab has formed on top of it. For this to be the case both the threshold of slab thickness of 0.18 m (Schweizer et al., 2008) and the threshold of average slab density of 100 kg/m^3 must be exceeded. The latter choice refers to typical values for slabs involved in avalanches which had hand hardness indices of at least 4F- (Schweizer and Jamieson, 2003) which corresponds to about 105 kg/m^3 for precipitation particles or 162 kg/m^3 for rounded grains (Geldsetzer and Jamieson, 2001). Provided a slab has formed, snow instability indicators are calculated for that weak layer and stored. Non-persistent weak layers, even if not relevant at the time of analysis, are tagged and remain one more day in the list of relevant weak layers. Persistent weak layers are not dropped from the list of relevant weak layers.

3.2. Weak layer tracking

Every day, tagged weak layers, i.e. layers that were identified on one of the previous days, are analyzed for their relevance (Fig. 2). To track weak layers, we use layer properties stored from the previous time step, including grain shape and depth, to identify these in the current time step. Tracking only by age can be ambiguous as layers can be merged in the models.

Weak layers are considered relevant to the instability of the snow cover when a sufficiently thick and dense slab – as described above – has formed. Such a slab can form soon after burial or after some more time. However, after 48 hours since burial without loading due to new snow or blowing snow, non-persistent weak layers are not considered for the following day, as with short-term strengthening of non-persistent weak layers natural dry-snow slab activity substantially decreases after a snowfall (Heck et al., 2019; Stoffel et al., 1998). This is consistent with typical life spans of non-persistent weak layers of 3 (Brown and Jamieson, 2008) to 4 days (Gauthier et al., 2010) after burial assuming that a storm lasts for one day at least. As persistent grain shapes strengthen more slowly (Jamieson, 1995), we consider a persistent weak

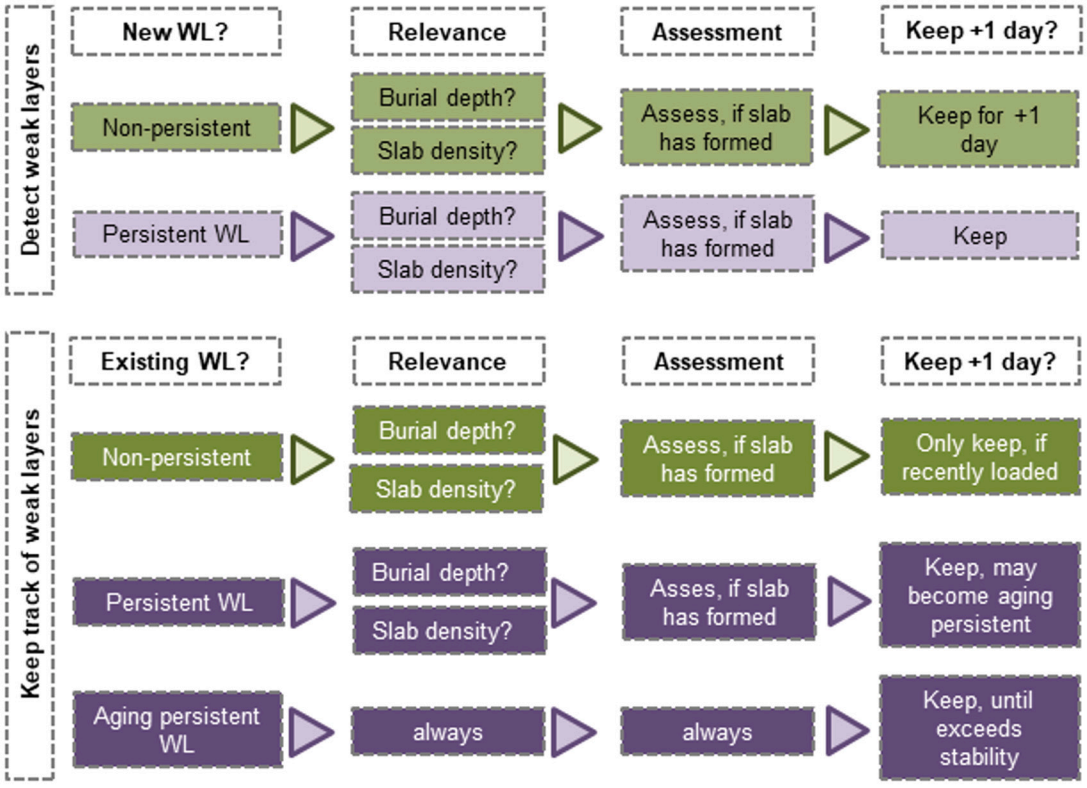

Fig. 2. Workflow for weak layer (WL) detection and weak layer tracking for weak layers with non-persistent and persistent snow grain shapes. Details of the snow instability assessment (3rd column) are given in (Fig. 3). The fourth column shows how long weak layers are kept for assessment.

layer as long as the layer includes persistent grain shapes.

When more snow accumulates during the winter season, persistent weak layers become more deeply buried in the snowpack. Then, artificial triggering of such persistent weak layers becomes unlikely due to their depth, and the algorithm moves the persistent weak layers to the category «aging» persistent weak layer based on the simulated snow instability indicators (next section). Aging persistent weak layers only play a secondary role: usually they are not triggered by an additional load such as new snow or skier loading. If, however, another weak layer above fails, this slab avalanche may initiate a second fracture in the aging persistent weak layer – potentially increasing avalanche size.

3.3. Release mechanisms and snow instability criteria

Following the concept of avalanche formation (Schweizer et al., 2016a), we selected snow instability indicators to assess the propensity for natural release and for artificial triggering. We favored easy to implement concepts that are applicable to standard snow cover models and have been shown to yield acceptable results at low computational cost. As avalanche release processes and field observations differ, we separate natural release and artificial triggering.

3.3.1. Natural release

To describe the natural failure initiation process, which starts with damage in the weak layer due to increasing overburden stress, we employ the stability index S_n and the expected time to failure t_f (Conway and Wilbour, 1999) which depend on weak layer strength, overburden stress and their rate of change. We compute the ratio $S_n = \tau_p/\tau$ that describes a balance between shear strength in the weak layer (τ_p) and additional shear stress due to the weight of the slab (τ) on an inclined slope of 38°. The ratio suggests that failure becomes more likely when values are low, theoretically as low as 1 (Perla and LaChapelle, 1970). Conway and Wilbour (1999) built on this concept and derived a related property, the expected time to failure t_f, which includes the time derivative of the stability index:

$$t_f\ (t) = \frac{S_n(t) - 1}{\frac{dS_n}{dt}}$$

and indicates instability when values decrease towards zero. Thresholds for instability are given in Table 1. We approximated the time derivative as change of the natural stability index per hour.

The critical crack length a_c describes the onset of crack propagation, which is the subsequent stage in the chain of events preceding avalanche release. To calculate the critical crack length a_c (Reuter and Schweizer, 2018) we derive the mechanical energy (Heierli et al., 2008) and solve for critical crack length (Schweizer et al., 2011) using finite element calibrations (van Herwijnen et al., 2016). The weak layer fracture was approximated from the simulated shear strength squared (Gaume et al., 2014). To omit finite element simulations we calculate an average slab modulus based on density and layer thickness. The criteria are calculated for non-persistent and persistent weak layers (Fig. 3).

To assess wet-snow conditions, we used the liquid water content index (Mitterer and Schweizer, 2013) in combination with the days since the isothermal state was reached (Baggi and Schweizer, 2009). The liquid water content is simulated for each layer of the snowpack as the amount of liquid water per volume of snow. The values are averaged accounting for layer thickness to obtain a liquid water content of the entire snowpack. The liquid water content index is the liquid water content of the entire snowpack divided by a critical liquid water content of 1% water volume per ice volume (Table 1) which is typical for matrix flow (Mitterer et al., 2016). If the liquid water content index reaches 1 for the first time, natural wet-snow avalanches are expected. We use the liquid water content index to determine the onset of the first wet-snow avalanche conditions in spring. In the period after the wet-snow avalanche onset we apply two rules: on one hand increasing liquid water content and on the other return to stability after 4 consecutive days of isothermal state (Baggi and Schweizer, 2009).

Table 1
Thresholds used for snow instability indicators derived from SNOWPACK and Crocus simulations for non-persistent and persistent weak layers and for wet-snow.

	Natural release		Artificial triggering	
	SNOWPACK	Crocus	SNOWPACK	Crocus
Natural stability index	3.6[a]	2.5[a]		
Expected time to failure (h)	18[a]	27[a]		
Critical crack length (m)	0.32[a]	0.36[a]	0.3	0.3
Critical liquid water content (% vol.)	1	1		
Days since isothermal state (days)	4	4		
Failure initiation criterion			1	1

[a] Thresholds derived in this study.

3.3.2. Artificial triggering

For dry-snow slab avalanche release, the propensity for artificial triggering can be described by the failure initiation criterion S and the critical crack length a_c (Reuter et al., 2015a). The failure initiation criterion is the ratio $S = \tau_p/\delta\tau$, which compares weak layer shear strength (τ_p) and the additional shear stress at the depth of the weak layer ($\delta\tau$) due to skier loading. The simulation of the additional shear stress at the depth of the weak layer is circumvented by using an analytical expression (Monti et al., 2016). Decreasing values indicate that failure initiation becomes more likely. We utilized the critical crack length as described previously (Reuter and Schweizer, 2018) with the thresholds summarized in Table 1.

The failure initiation criterion and the critical crack length are calculated for non-persistent, persistent and aging persistent weak layers – contrary to natural release where natural stability index and expected time to failure are computed instead of the failure initiation criterion.

3.3.3. Thresholds for snow instability indicators

To decide if a slab/weak layer combination is stable or unstable, we use thresholds for the snow instability indicators (Table 1). Thresholds for natural release of dry-snow were derived in this study and are presented in the section Results. For artificial triggering, we use the threshold $S < 1$ for the failure initiation criterion and $a_c < 0.3$ m for the critical crack length. Both indicators have been used by Reuter and Schweizer (2018). They had determined a threshold $S < 200$, whereas here we use a threshold of $S < 1$ which means that the stress due to an additional load is larger than the strength in the weak layer. The difference is related to strength estimates from snow-micro penetrometer measurements, which are higher than typical values of snow shear strength (Marshall and Johnson, 2009). As the snow cover model simulated strength values are of the right order of magnitude, we can use $S < 1$ for failure initiation. For crack propagation, we used the reported threshold of $a_c < 0.3$ m.

We changed a persistent weak layer into an aging persistent weak layer if the failure initiation criterion reached $S > 2$ or the critical crack length reached $a_c < 0.6$ m, since in Reuter and Schweizer (2018) signs of instability were absent when the threshold value doubled.

3.4. Identifying avalanche problems

3.4.1. Natural release

Non-persistent weak layers fail in new snow or drifting snow situations, when precipitation rates exceed weak layer strength (Perla and LaChapelle, 1970). Hence, loading is required, but since the amount of new snow is not entirely sufficient to explain natural avalanche activity (Schweizer et al., 2009), we also need to consider snow instability indicators to describe the conditions in the weak layer. We identify a new

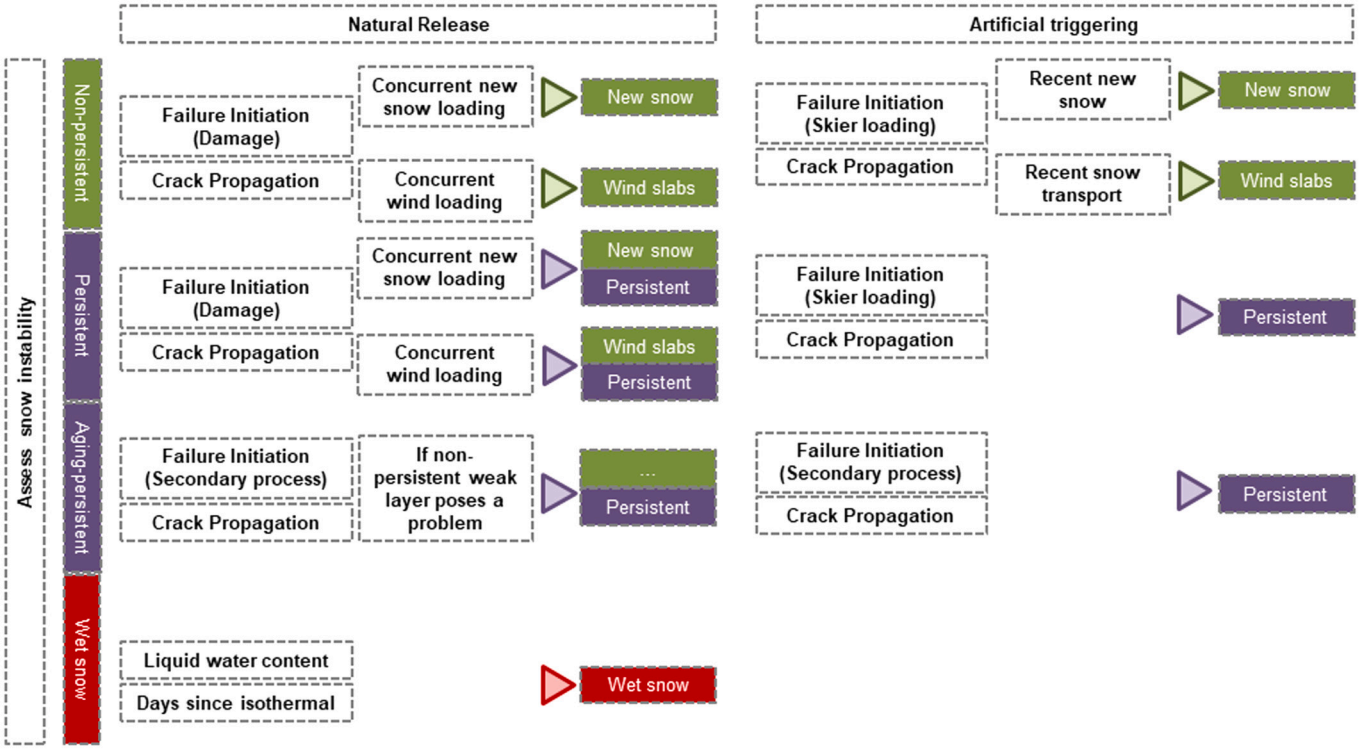

Fig. 3. Snow instability assessment and avalanche problem selection for weak layers underlying a potential slab. Modelling steps include failure initiation and crack propagation for dry-snow. Failure initiation considers new snow loading leading to weak layer damage for natural release and additional external loading due to a skier for artificial triggering. New snow or wind loading indicators are required to conclude on the different avalanche problem types.

snow problem or a wind slab problem when:

- a non-persistent weak layer and a relevant slab
- are loaded by new snow or drifting snow (thresholds in Table 2), respectively, and
- snow instability indicators become critical in this weak layer for natural release (Table 1).

We distinguish between new snow and wind slab problems based on weather variables. In case new snow was recorded, it is considered a new snow problem. With indication of snow transport the wind slab problem is chosen. The new snow and the wind slab problem may co-exist.

Persistent weak layers form due to temperature gradients in the snowpack during periods of clear and calm weather (Birkeland, 1998; Colbeck, 1988). Only after burial and with sufficient loading from new or blown snow, these weak layers may fail and create an avalanche (McClung, 1981). We consider preexistence, loading and instability, and identify a persistent weak layer problem when:

- a persistent weak layer and a relevant slab
- are loaded by new snow or drifting snow (thresholds in Table 2) and
- snow instability indicators become critical in this weak layer for natural release (Table 1).

Table 2
Thresholds used to identify avalanche problem types.

	SNOWPACK	Crocus
Min. amount of new snow (m/24 h)	0.05	0.05
Height of snow drifts (m/24 h)	0.4	
Saltation mass transport rate (kg/cm/24 h)		0.2
Liquid water content (% vol.)	1	1
Days since isothermal state	4	4

Obviously, often this situation of a persistent weak layer will coincide with the new snow or the wind slab problem. However, loading can be sufficient to activate a persistent weak layer without forming a critical non-persistent weakness. In addition, we also identify a situation as a persistent weak layer problem, when an aging persistent weak layer is present and a new snow or wind slab problem was identified.

Natural avalanches may also release due percolating water (Conway et al., 1989). When the liquid water content index reaches 1 the spring wet-snow avalanche cycles set in. From this date we identify a wet-snow problem, if:

- the liquid water content in the snowpack has increased from the previous day, but
- for no longer than 4 subsequent days since the last time the snowpack became isothermal (Baggi and Schweizer, 2009).

3.4.2. *Artificial triggering*

New snow or drifting snow situations can be prone to artificial triggering (e.g. Gauthier et al., 2010). We consider it a new snow / wind slab problem, if:

- a non-persistent weak layer and a relevant slab exist and
- snow instability indicators for skier triggering fall below thresholds (Table 1).

We distinguish between new snow and wind slab problems as previously described. They may co-exist.

Skier triggering is typical with persistent weak layers, although less so with aging persistent weak layers (Marienthal et al., 2015). We select the persistent weak layer problem, if:

- a persistent weak layer and a relevant slab exist and
- snow instability indicators for skier triggering fall below thresholds (Table 1).

In addition, we also identify a situation as a persistent weak layer problem, when an aging persistent weak layer is present and a new snow or wind slab problem was identified.

3.4.3. Thresholds for avalanche problems

The first threshold in Table 2 represents the minimum value required for loading by new snow. With at least 5 cm of new snow recorded within 24 h we consider that a new snow problem may exist or persist. To pick out many potential situations we set rather low thresholds. The wind slab threshold refers to a theoretical concept and values do not represent a realistic situation. With a value of 40 cm/24 h, for instance, we should not expect 40 cm deep snow drifts, but rather less. The last two thresholds refer to wet-snow situations.

3.5. Statistical evaluation of results

We use statistical metrics to assess the performance of avalanche problem identification and to assess a useful combination of snow instability indicators for natural release.

To assess the accuracy of classifying avalanche days we use the probability of detection (POD; also called true positive rate TP), the probability of correctly predicting days without avalanches or avalanche problems (PON) and the false alarm rate (FP = 1 − PON; also called false positive rate). The mean of POD and PON is called unweighted average accuracy (RPC) (Schweizer and Jamieson, 2010; Wilks, 2011).

To find a combination of snow instability indicators describing conditions conducive to natural release, we graphed predictions of avalanche days or avalanche problems using receiver operating characteristics (ROC) (Fawcett, 2006), which depicts the tradeoff between hits and false alarms and allows comparing models with different classifiers. The model scores, i.e. the probability that an observation belongs to the "unstable" class, were derived from the class proportions at the leaves of a classification tree (Breiman et al., 1998). The trees classified situations by optimizing the misclassification cost. Classification trees had a maximum of 2 splits per predictor variable. The Gini coefficient (GINI) is a measure of classification quality and relates to the area between the ROC curve and the 1:1 line. The point on the ROC curve at maximum distance perpendicular from the diagonal corresponds to the probability threshold yielding the highest value of the true skill statistic (TSS=POD−FP, Wilks, 2011).

Moreover, we use Pearson's correlation coefficient and p-value to test the strength and significance of a relationship.

4. Results

We describe one avalanche situation to explain how the algorithm works. Then, we present simulated snow instability indicators obtained from SNOWPACK and Crocus simulations at Weissfluhjoch, Davos. Comparing the data with monitored natural avalanches we derive snow instability thresholds for natural release which ultimately allows us to assess the avalanche problem types. Applying the thresholds to snow cover simulations we can characterize avalanche problems at three different locations and in the cases of two Canadian stations compare modeled and observed avalanche problem types.

4.1. Weak layer detection and tracking during an avalanche cycle at Weissfluhjoch, 26 December 2014 to 2 January 2015

During the last days of December 2014, an interesting avalanche situation with two different weak layers occurred and detailed field records from the area around the Weissfluhjoch study plot were available. From 26 December to 31 December a total 42 cm of snow accumulated at Weissfluhjoch. During this period, a persistent weak layer consisting of facets and a non-persistent weak layer consisting of decomposing and fragmented particles were observed in manual snow profiles (Fig. 4).

Compression and extended column test results showed failures in both weak layers during this period. Field observers reported natural release and remote triggering. In fact, two of the three snow pits were dug near triggered avalanches and explain that triggering was possible on both weak layers. Several natural and artificial avalanches were observed in the period between 30 December and 1 January (Fig. 5).

In the SNOWPACK simulations, both weak layers were identified and tracked. The stability indicators show that conditions were susceptible for natural release, in particular between 30 December 6:00 and 31 December 6:00 when the minimum time expected to failure in the non-persistent weak layer was only 45 min. A total of 15 natural avalanches were recorded on 31 December and another 14 on 1 January with mostly uncertain release times. Stability indicators for artificial triggering were low in both weak layers from after weak layer burial until the end of the described period. Values of the failure initiation criterion were around 1 indicating that the additional load of a skier could induce a shear stress in the weak layer of the same magnitude as the weak layer's shear strength. Lowest values of the critical crack length were around 30 cm, which is a typical value associated with instability as comparisons with avalanche activity index (Schweizer et al., 2016b) or other stability results (Calonne et al., 2020) have indicated. Avalanche control work released avalanches mainly after the storm on 31 December. Skier-triggering was common in the entire period and peaked on 1 January, when good skiing conditions and fair weather attracted skiers.

The tracked weak layers in the SNOWPACK simulations and the derived stability indicators agreed well with the observed weaknesses that contributed to the instability during the described avalanche cycle at the Parsenn resort around Weissfluhjoch. The period between 30 December and 1 January shown in Fig. 5 also illustrates that tracking the weak layer facilitates interpretation. Using a single classifier to identify the weak layer, take for instance an expected time to failure $t_f < 14$ h, the non-persistent weak layer would be relevant on 30 December, 31 December and 1 January and the persistent weak layer would be relevant on 31 December and 1 January. We miss information if we report only the layer with the poorest stability result: a non-persistent weak layer on 30 December, a non-persistent weak layer on 31 December, and persistent weak layer on 1 January. Apparently, both weak layers contributed the situation (the non-persistent and the persistent weak layer), so both need to be evaluated – which will be important in particular for avalanche problem assessment.

4.2. Snow instability indicators at Weissfluhjoch during winter season 2015–16

To assess natural release during the period with dry-snow conditions (before 31 March 2016 in that season) we calculated three snow instability indicators. The natural stability index, the expected time to failure and the critical crack length were computed for new snow problems and for persistent weak layer problems, i.e. when a non-persistent weak layer was loaded by new snow or when a persistent weak layer was loaded with new snow, respectively. Comparing the indicators with observed natural avalanches allows us to determine thresholds for each of the three snow instability indicators.

We only considered days as potential days with dry-snow natural release, if a weak layer was present in the snow cover simulations (non-persistent or persistent) and additional loading occurred ($N = 56$ in the season 2015–16). From the first splits in classification trees, the following instability thresholds were obtained: the natural stability index ($S_n < 3.6$) identified 47% of the days with natural avalanches, the expected time to failure ($t_f < 18$ h) 87% of the avalanche days and the critical crack length ($a_c < 0.28$ m) 73% of the avalanche days based on SNOWPACK simulations (Table 3). With Crocus simulations the natural stability index ($S_n < 2.5$) identified 39% of the avalanche days, the expected time to failure ($t_f < 27$ h) 77% of the avalanche days and the critical crack length ($a_c < 0.37$ m) detected 85% of the avalanche days. Except for the natural stability index, the POD values of the single

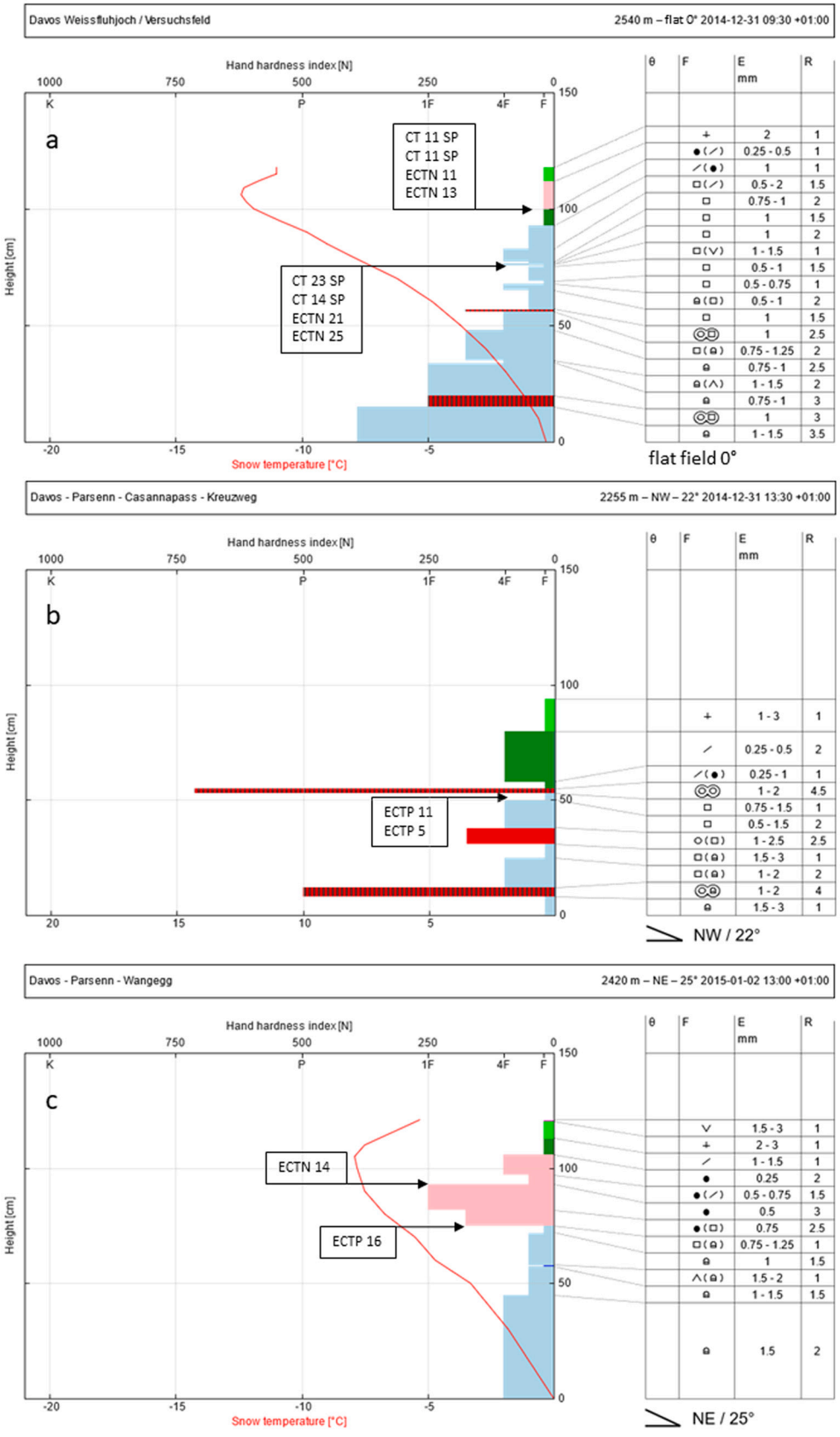

Fig. 4. Three snow profiles from 31 December 2014 (a) and 2 January (b, c) observed in the Parsenn resort around Weissfluhjoch. Stability test results are given for two weak layers: a non-persistent weak layer in the more recent accumulation and a persistent weak layer further below. Both weak layers were identified in all three pits. Two pits show failures on the non-persistent weak layer. All three pits show failures on the persistent weak layer.

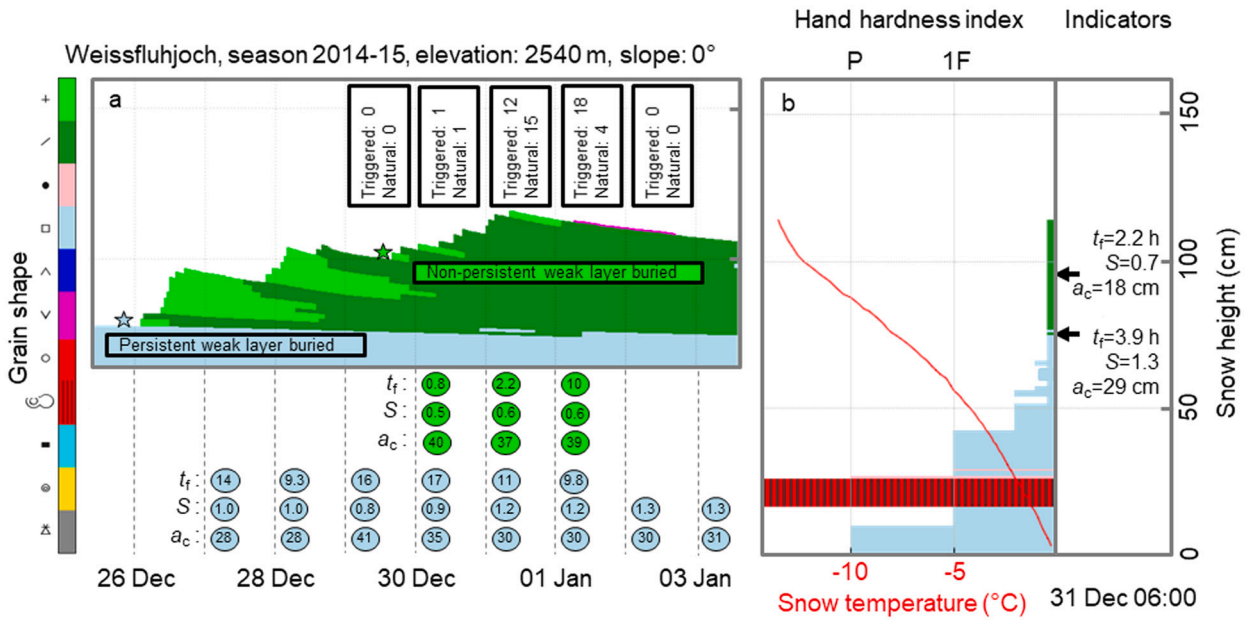

Fig. 5. (a) Snow cover simulation with SNOWPACK showing two weak layers that were detected and tracked between 26 December 2014 and 3 January 2015. During several storms the simulated snow height increased from 74 cm on 26 December to 115 cm on 31 December 2014. Simulated stability indicators are shown for both weak layers and include expected time to failure t_f, failure initiation criterion S and critical crack length a_c. Snowpack layers deeper than 65 cm are not shown. Between 30 December 2014 and 1 January 2015 ski patrol observed numerous naturally and artificially released avalanches in the Parsenn resort around Weissfluhjoch. (b) Simulated snow profile on 31 December 2014 at 06:00 with hand hardness index, snow temperature, grain type and snow instability indicators including expected time to failure t_f, failure initiation criterion S and critical crack length a_c for both weak layers.

Table 3
Probabilities of detecting avalanche days (POD) and non-avalanche days (PON) and accuracy (RPC) for snow instability thresholds for natural release derived from classification trees.

Snow instability indicator	SNOWPACK			Crocus		
	POD	PON	RPC	POD	PON	RPC
Natural stability index	0.47	0.68	0.57	0.39	0.96	0.67
Expected time to failure (h)	0.87	0.61	0.74	0.77	0.04	0.41
Critical crack length (m)	0.73	0.32	0.53	0.85	0.54	0.69
Liquid water content and < 5 days since isothermal state	0.5	0.45	0.48	0.60	0.65	0.62

The thresholds were applied to SNOWPACK and Crocus snow cover simulations and results compared to observed natural avalanches.

classifiers were higher than the PON values, which describe the probability of picking out the non-avalanche days correctly. Given that there is no single best classifier, we try combinations of the classifier below in section 5.3.

To determine the onset of the first wet-snow avalanche conditions in spring we calculated the liquid water content index. After the onset our model anticipates wet snow avalanches with increasing liquid water content and return to stability after 4 consecutive days of isothermal state (Baggi and Schweizer, 2009). We obtained an accuracy of estimating wet-snow avalanche days after the onset date (31 March 2016) of RPC = 0.48 (POD = 0.5; PON = 0.45) with SNOWPACK simulations and an accuracy of RPC = 0.62 (POD = 0.6; PON = 0.65) with Crocus simulations. The results are balanced with similar values of POD and PON.

4.3. Combining snow instability indicators for natural dry-snow avalanche release

Having derived thresholds for single classifiers, we now combine two classifiers, as research of dry-snow avalanche release suggests that two criteria – one for failure initiation and one for crack propagation – allow for a more accurate assessment of instability. Hence, we complement the

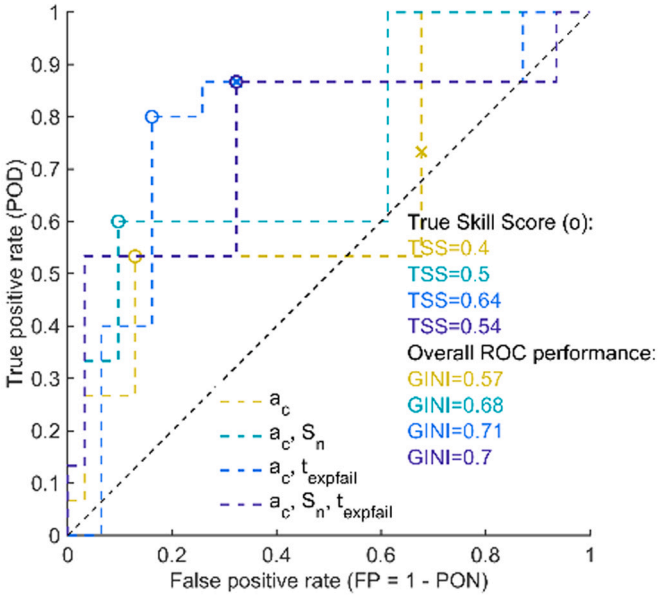

Fig. 6. Avalanche days in ROC space as predicted by snow instability indicators derived from the SNOWPACK simulations for days with non-persistent or persistent weak layers prone to natural release (definitions in section 4). Indicators include the critical crack length a_c the natural stability index S_n and the expected time to failure t_f. Scores were calculated from classification trees. Colors indicate combinations of indicators. Circles indicate the highest value of TSS i.e., best prediction of the classification tree. The GINI coefficient summarizes overall performance of the classification tree. Classification with a single threshold $a_c < 0.28$ m by yellow cross. Classification with $t_f < 18$ h and $a_c < 0.32$ m by blue cross. (References to colour in the figure legend, or in the web version of this article.)

critical crack length with one of the failure initiation criteria for natural release and graph the results as receiver operating characteristics (ROC) in Fig. 6 for the SNOWPACK simulation of the 2015–16 season at Weissfluhjoch. As before, days were considered as potential avalanche days if a weak layer was present (non-persistent or persistent) and loading occurred due to new snow or drifting snow. The ROC curves depict the tradeoff between identifying avalanche days (if the true positive rate is high) and correctly classifying non-avalanche days (if the false positive rate is low). The yellow ROC curve in Fig. 6 represents different thresholds when the critical crack length is used as a single classifier. The higher the threshold of the critical crack length is chosen, the more avalanche days are detected (increasing TP rate), but the less specific the classification is with respect to non-avalanche days (also increasing FP rate). In other words, increasing the threshold of the critical crack length means movimng along the yellow line from the lower left to the upper right on the graph. Using the threshold determined from the classification tree $a_c < 0.28$ m is a conservative choice, with a high probability of detecting avalanche days (11 out of 15 days; POD = 0.73), but misclassifying about two thirds of the non-avalanche days (21 out of 31 days; FP = 0.68).

Combining the critical crack length with the natural stability index improves the accuracy slightly according to the true skill score TSS = 0.5, which was higher than for the single classifier critical crack length (TSS = 0.4). Combining the critical crack length with the expected time to failure t_f yielded TSS = 0.64 – indicating higher predictive power. The improvement comes with an improved prediction of non-avalanche days which is reflected in a false positive rate of 0.16 (i.e. PON = 0.85) and with a POD that increased from 0.53 to 0.8. The improvement is also reflected in the GINI coefficient which increased from 0.57 to 0.71. Combining all three indicators did not improve the prediction. In fact, two thresholds, one for the expected time to failure $t_f < 18$ h and one for the critical crack length $a_c < 0.32$ m identify days with natural avalanche release with a probability of more than 87% (light blue cross) at a false alarm rate of 32%. We use these two thresholds to assess natural release and eventually the corresponding avalanche problem types in SNOWPACK simulations (Table 1).

Using Crocus snow cover simulations for the same season 2015–16 also showed that a combination of expected time to failure and critical crack length can separate avalanche from non-avalanche days fairly well (TSS = 0.69; GINI = 0.76). Combining the expected time to failure $t_f <$ 27 h and the critical crack length $a_c < 0.36$ m yielded a satisfying classification based on two single classifiers only (POD = 0.70; FP = 0.33) that we can use to assess natural release and eventually the corresponding avalanche problem types in Crocus simulations (Table 1). As expected, time to failure and critical crack length are used in combination, threshold values differ from typical values when the indicators are used alone, such as natural stability index $S_n = 1$.

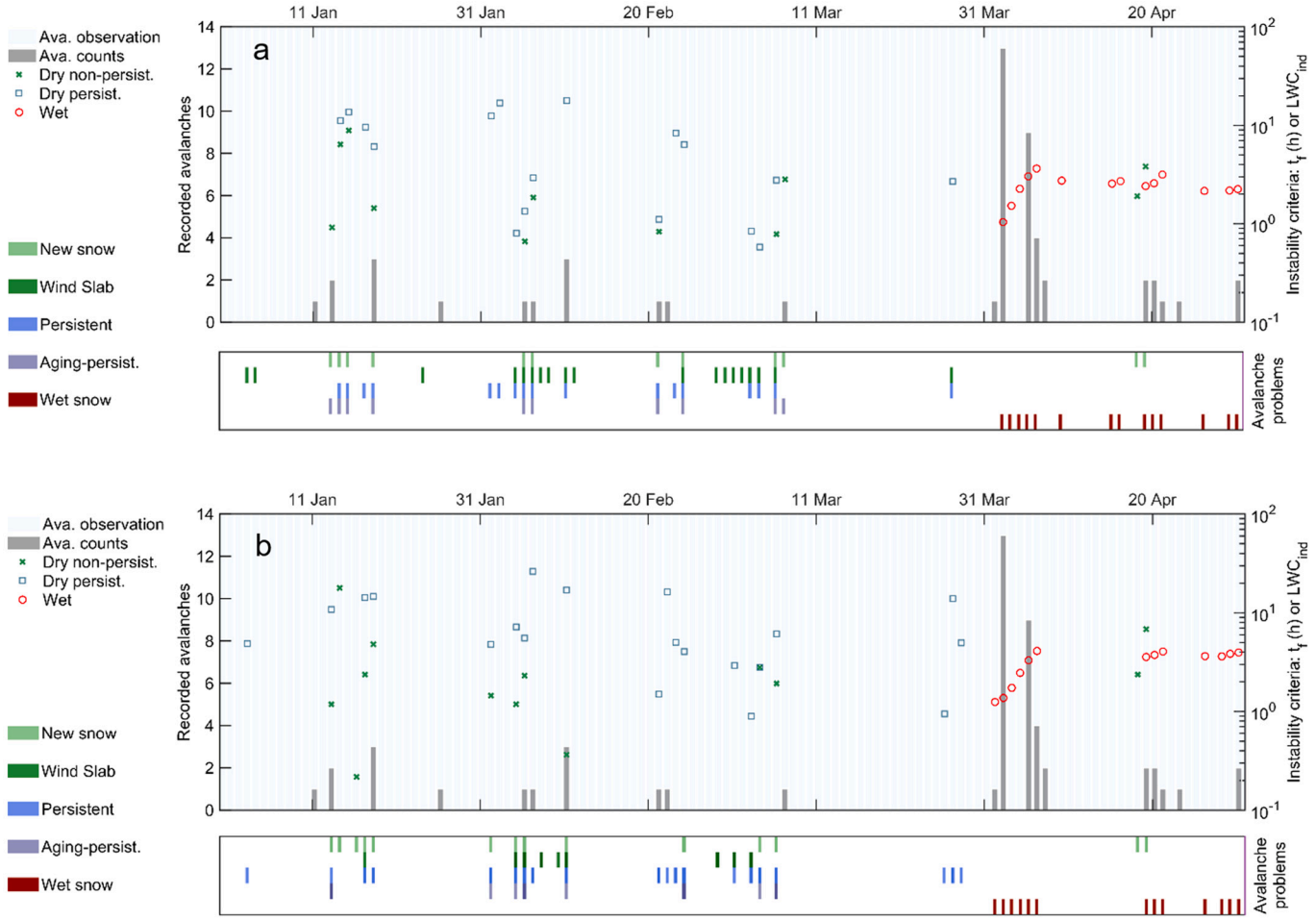

Fig. 7. Number of avalanches per day in the seismic avalanche catalogue (gray bars) are shown. Seismic observations were available for the shown period (blue background). Simulated avalanche problem types for natural release from 01.01.2016 to 30.04.2016 based on (a) SNOWPACK and (b) Crocus simulations at Weissfluhjoch, Davos. Expected time to failure t_f is graphed for non-persistent (green crosses) and persistent weak layers (blue squares) that relate to new snow (light green bars) or persistent weak layer problems (light blue bars) promoting natural snow instability. Dark green bars denote wind slab problems. Values of liquid water content index LWC_{ind} (red circles) are shown for all days when wet-snow problems were identified (red bars). Problems related to aging persistent weak layers by dark blue bars. (References to colour in the figure legend, or the is referre t the web version of this articl

4.4. Avalanche problems and natural activity at Weissfluhjoch during winter 2015–16

We compare the natural avalanche activity during the winter season of 2015–16 to simulated avalanche problems that are related to natural release.

Fig. 7 shows the number of avalanches per day from the seismic avalanche catalogue. Data were recorded from 1 January 2016 until 30 April 2016 without interruption (period presented in the figure). The first part of the winter season shows several avalanche cycles with up to three avalanches per day, whereas from the beginning of April daily avalanche activity was higher with up to 13 avalanches per day.

At the bottom of Fig. 7 a and b, colored bars indicate the simulated avalanche problem types in view of natural release for each day. We assumed that the snow cover was prone to natural release when both the expected time to failure and the critical crack length were below thresholds (Table 1). In other words, the indicated avalanche problems correspond to one or more weak layers that are critical for natural release. The expected time to failure of those weak layers is shown in the upper part of the graph with a symbol denoting weak layer type.

For example, on 17 January three avalanches were recorded and a new snow problem with a non-persistent weak layer was identified in the SNOWPACK simulations. The non-persistent weak layer had critical stability with an expected time to failure of $t_f = 1.8$ h and a natural stability index of $S = 2.2$ on 17 January at 14:00. That means, if the conditions on 17 January at 14:00 had continued for another 1.8 h, the natural stability index would have decreased to 1. Hence, during this period stability decreased to a poor level which is indicated by the trend (expected time to failure) and the degree of the instability (natural stability index). In addition, a persistent weak layer was present in the snow cover with an expected time to failure of $t_f = 6.6$ h. The Crocus simulation also produced a non-persistent and a persistent weak layer. The expected times to failure were lowest on 17 January at 3:00 and were 3.2 h and 11.2 h for the non-persistent and the persistent weak layer, respectively. This minimum of stability coincides with three avalanches that were detected between 00:00 and 03:00 on 17 January.

The presented approach to assess avalanche problems provides a means to link simulated snow profiles to observed snow instability, which in our case is avalanche activity.

4.5. Frequency of avalanche problem types during periods with natural release at Weissfluhjoch for the season 2015–2016

The frequency of avalanche problem types estimated by the models is summarized in Table 4 – along with the number of avalanche days in the seismic avalanche catalogue.

The number of days that the two snow cover models identified a new snow or a persistent weak layer problem were similar. On about every second or third days with an identified new snow or persistent weak layer problem natural avalanches were also observed. In the cases that drifting snow was the expected problem, results varied considerably. Only every fifth to seventh day avalanches were actually observed, which probably comes from the simplifications in the model.

Table 4
Frequency of avalanche problem types between 18 December 2015 and 31 May 2016 at Weissfluhjoch based on snow cover simulations with SNOWPACK and Crocus and number of days when natural avalanches were observed concurrently.

Avalanche problem	SNOWPACK	Avalanche days	Crocus	Avalanche days
New snow	13	7	14	5
Wind slabs	20	3	9	2
Persistent weak layer	17	7	20	7
Wet-snow	22	8	17	8

During the wet-snow season, we identified more days with a wet snow avalanche problem in SNOWPACK simulations (22 days) than in Crocus simulations (17 days). Again, only about every second or third day natural avalanches were also recorded.

4.6. Avalanche problems at Weissfluhjoch, Davos: Time series from 1999 to 2016

Fig. 8 shows SNOWPACK and Crocus model results at Weissfluhjoch from 1999 to 2016 in terms of the frequency of avalanche problem types. Every day, up to 4 avalanche problem types were identified. The time series shows how often a certain problem type was relevant during the winter season. New snow, wind slab, persistent weak layer and wet-snow problems appeared in both simulations across all winter seasons. The number of days per season when models suggested natural release varied between 20 and 52 for SNOWPACK and between 28 and 50 for Crocus. In some winters problem types overlapped more than in others. In other words, there are seasons with many problem types on rather few potential avalanche days. For instance, for the winter of 1999–2000 SNOWPACK counted 67 avalanche problem types on 38 days, while the season of 2010–2011 had only 48 problem types spread over 37 days. With Crocus 71 problem types were selected on 50 days in 1999–2000 and in 2010–2011 42 problem types on 35 days.

There is some agreement between the results obtained from SNOWPACK and Crocus simulations how seasons with many problems alternate with seasons with fewer problems. The number of avalanche problem types per season were correlated ($r = 0.70$, $p < 0.01$). Besides, the number of days that the two snow cover models anticipated natural release agreed fairly well ($r = 0.61$; $p = 0.01$). Only in the three winter seasons of 2000–2001, 2008–2009 and 2011–2012 the number of avalanche days the two models estimated were larger than 20%.

The onset of the first wet-snow avalanche cycle in spring shifted during the 16-year period by about 2 weeks if the onset dates are smoothed with a 10-year moving average. A 10-year moving average revealed a significant increase in the frequency of wind slab problems in SNOWPACK simulations ($p = 0.01$). This trend was not present in Crocus simulations that estimated about 9–10 days with wind slab problems per season on average. The number of days with wet-snow problems seemed to slightly increase over the period, but the trend was not significant, neither in SNOWPACK ($p = 0.1$) nor in Crocus simulations ($p = 0.3$). New snow and (aging-)persistent weak layer did not show trends with neither snow cover model.

The pie charts reflect the snow climate observed during the period of 16 years. Both snow cover models showed similar proportions of (aging-)persistent weak layer problems (37% or 31%) and wet-snow problems (22% or 21%). The proportion of new snow and wind slab problems account for almost half of the problem types according to the two simulations (41% or 47%). The proportion of days with (aging-)persistent weak layer problems seem characteristic of an intermountain snow climate (Mock and Birkeland, 2000).

4.7. Avalanche problems in Western Canada: A 5 winters' time series

Fig. 9 shows simulated and observed avalanche problem types for the winter seasons between 2015 and 2020 at Whistler, BC and Rogers Pass in Glacier National Park, BC. An observed storm snow problem corresponds to the simulated new snow problem (green), the observed persistent slab problem to the persistent weak layer problem (blue), the deep persistent slab problem to the aging persistent weak layer problem (dark blue), a wet slab problem to the wet-snow problem (red).

Observations from Whistler show that during the observation period between 1 December and 1 April, avalanche problems were mostly new snow problems: 22 days per season on average according to observations or 19 days per season on average according to the model. The second most common avalanche problem type was the persistent weak layer problem with 9 days on average, based on either data. In the snow cover

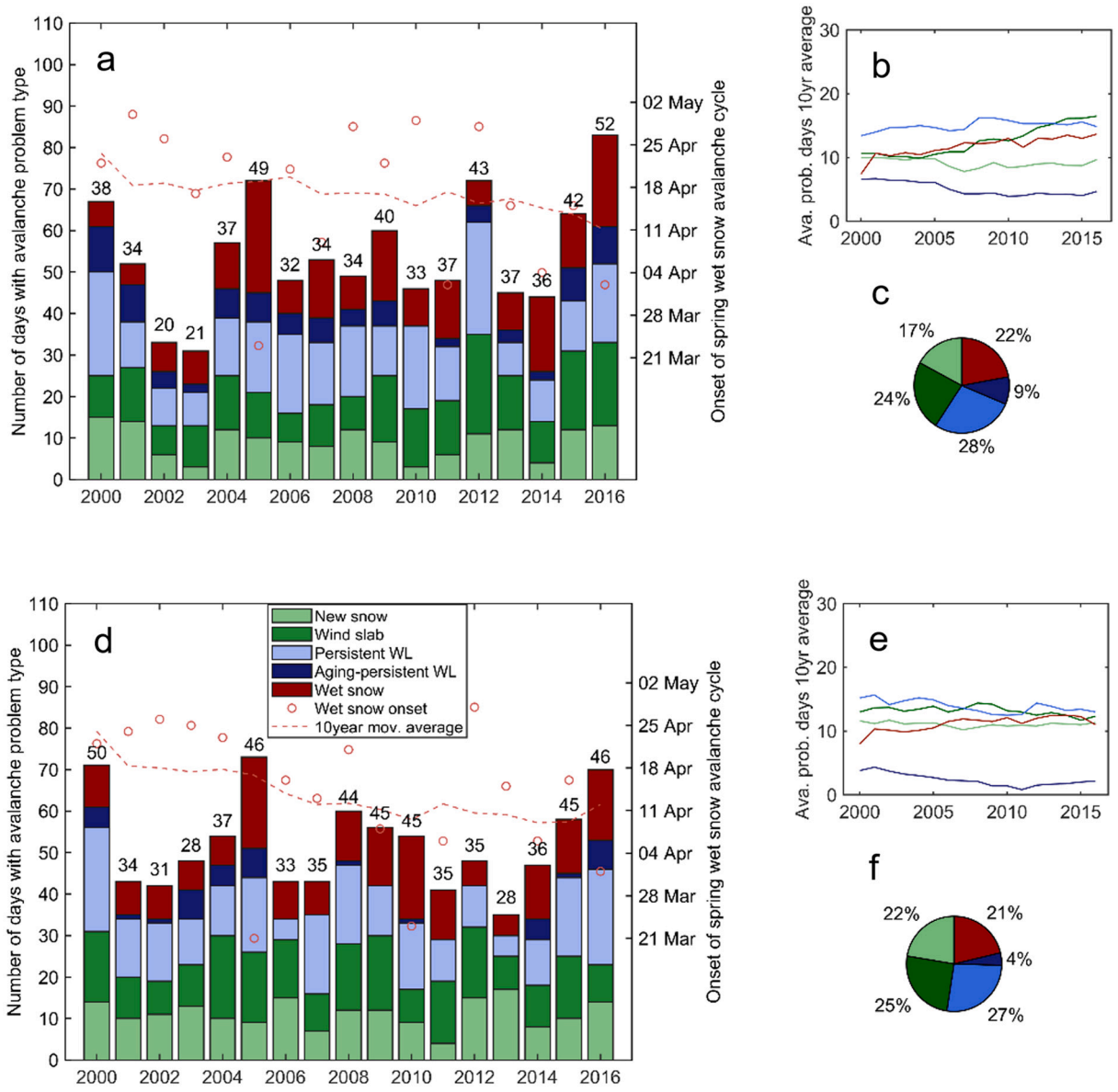

Fig. 8. Avalanche problem types derived from (a,b,c) SNOWPACK and (d,e,f) Crocus simulations for the winter seasons from 1999 to 2016. Stacked colored bars illustrate the occurrence of avalanche problem types for different seasons (a,d). Number of avalanche days above the bars. Red circles denote the onset of the first wet-snow avalanche cycle in spring and a dashed line shows the 10-year moving average of this date. 10-year moving averages also illustrate the temporal evolution avalanche problem type occurrences (solid lines in b and e). Pie charts summarize the occurrence of avalanche problem types in the entire period (c,f). References to colour in the figure legend, or in the web version of this article.

model data the same avalanche problems dominated as in the observations. A closer look into the seasons reveals, that from the simulations few wet-snow avalanche problems were identified in all seasons except for 2019–2020. Observation records have wet-snow problems in 2015–2016 on a few days (one cycle after 29 November 2015 and another one after 21 January 2016). We may expect the wet-snow avalanche problem type to be more frequent, because wet-snow avalanche activity is common in the mountains around Whistler. However, our data end 1 April and thus do only partly cover the late part of the season when wet-snow problems are usually more common. So, our data does not fully represent the snow climate of Whistler.

Observed avalanche problem types at Rogers Pass suggest that persistent weak layer problems are more prevalent than new snow problems. Our modelling approach provided the same picture. Deep persistent slab avalanche problems were only reported in two seasons, whereas the models deem aging persistent weak layers more relevant. For observers, the distinction between persistent and deep persistent slab avalanche problems is difficult to make with current definitions. If we merge both problems involving persistent weak layers, there is better agreement in the observations and the simulated data. On average Rogers Pass had 66 days with avalanche problems related to persistent weak layers per season based on observations or 48 days based on the modelling approach. Wet-snow problems were neither simulated nor observed and are probably underrepresented as our data end 1 April.

Observations and modelling results highlight the differences between the snow climates at Whistler and Rogers Pass (pie charts in Fig. 9): Over the assessment period in Whistler new snow problems were on average twice as common as persistent weak layer problems according to the observations and the model. At Rogers Pass persistent weak layer problems were on average 5 times more frequently observed or modeled than new snow problems. Comparing the two locations, Whistler had twice as many days with avalanche problems related to

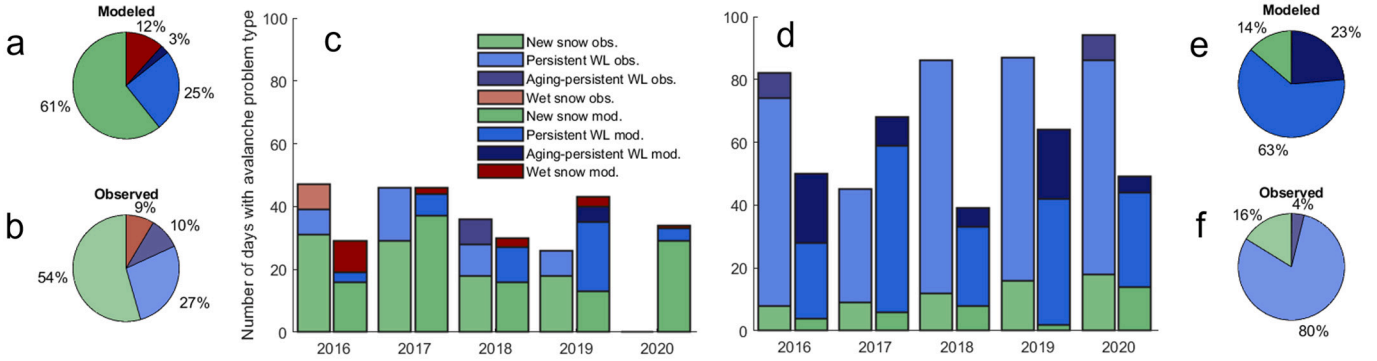

Fig. 9. Avalanche problems derived from numerical weather prediction data with SNOWPACK simulations for the winter seasons between 2015 and 2020 for Whistler (a,b,c) and Rogers Pass (d,e,f). Different colors denote avalanche problem types, with higher transparency for observed than for simulated data. Stacked bar graphs show the occurrence of the different avalanche problem types for each season (c,d). Pie charts summarize the frequency of the avalanche problem types over the entire period for Whistler (a,b) and for Rogers Pass (e,f). References to colour in the figure legend, or in the web version of this article.

new snow; 19 to 7 according to observations or 22 versus 13 according to modelling, respectively. Rogers Pass, on the other side, had about six times more days with avalanche problems related to buried persistent weak layers; 67 versus 10 as for the observations and 48 versus 10 as for the model results. In this example, the demonstrated approach discriminated between the avalanche problems typically observed in a coastal and an intermountain snow climate.

5. Discussion

Avalanche danger is usually described by its level (on a 5-level scale) and its characteristics (EAWS, 2021; Statham et al., 2018). Danger characteristics can be summarized and are increasingly communicated using the avalanche problem types. To assess avalanche problem types and describe the avalanche situation, we detected, tracked and assessed weak layers based on snow cover model data. First, we explained how we identify weak layers and assess snow instability for a situation that is well documented by field observations. We detected weak layers when they formed and followed them when they were buried. The present approach is not specific to snow cover model output, nonetheless predictions depend on temporal and vertical (snow layers) resolution of the employed snow cover model. We had 1 hour temporal resolution for meteorological data and about 50 layers in snow profiles. Our current approach may miss weak layers that develop within the snow cover due to temperature gradient metamorphism, as we scan the layers around the snow surface prior to the recent snow fall. Basal depth hoar, as an example, however, is not a common weak layer (Birkeland, 1998). Moreover, we only flagged wind slab situations rather than simulated actual additional loading due to snow transport by wind or potential weak layer formation within snow drifts.

5.1.1. *Snow instability indicators*

We used snow instability indicators to assess if a weak layer that we detected represented a critical weakness. We selected snow instability indicators based on the concepts of slab avalanche release (Schweizer et al., 2016a) and used either thresholds reported in earlier work or determined thresholds using an avalanche catalogue obtained with seismic monitoring.

Preceding natural release, deformation in the snowpack initially takes place at lower rates and a balance between healing of broken bonds and viscoelastic load redistribution determines stability (Capelli et al., 2018). Conway and Wilbour (1999) suggested a simplification of this concept and simulated the time to failure based on a balance between loading rate due to precipitation and weak layer strength gain to forecast the likelihood of natural release. We used their indicator to describe the natural failure initiation process. For natural release we complemented this criterion with the critical crack length, which was indicative of the crack propagation propensity in comparisons with observed signs of instability (Reuter et al., 2015a). We also assessed the predictive power of the natural stability index. However, the expected time to failure turned out a better discriminator when comparing with naturally released avalanches – both, as a single criterion and in combination with the critical crack length. Similarly, Brown and Jamieson (2008) found the expected time to be useful, as it describes the trend of snow instability during a snowfall event, which seems more appropriate for forecasting natural release than critical values of stability indices (Jamieson et al., 2007). We are aware that other formulations of the stability index (Lehning et al., 2004) or the critical crack length (e.g. Richter et al., 2019) are available, but exhaustive testing of other criteria is beyond the scope of this work. Our aim here was to use concepts that are applicable to most snow cover models and yield satisfactory results at low computational cost.

Snow instability estimates were computed from snow mechanical properties. Depending on the parametrization that is used in the snow cover model, critical values, such as the value of 1 for the natural stability index, may require calibration. For the two snow cover models we used, thresholds for natural release were 3.6 for the natural stability index from SNOWPACK and 2.5 for Crocus data, which means that layer properties are different in the snow cover models. Nonetheless, both models did similarly well at estimating days with natural dry-snow avalanche release – in particular when the expected time to failure and the critical crack length were combined. Regarding artificial triggering, we also used two criteria, the failure initiation criterion and the critical crack length as suggested by Reuter and Schweizer (2018), but omitted the finite element simulations that would be required for the tensile criterion. Contrary to natural release, we did not determine threshold values for instability. Data to do so are rare, as snow cover simulations would be needed for the location and time when snow instability data are available. Records of triggered avalanches, such as ski patrol records at Weissfluhjoch, only poorly reflect stable conditions because terrain use is not constant. Hence, we assessed instability with the following thresholds: Failure initiation was assumed if the failure initiation criterion $S < 1$ indicating that the stress due to an additional load is larger than weak layer strength. Moreover, we required critical cracks shorter than 0.3 m – a value typically observed with instability (e.g. Calonne et al., 2020; Schweizer et al., 2016b), which is compatible with the thresholds we determined with the seismic avalanche catalogue for natural release (0.32 m for SNOWPACK and 0.36 m for Crocus). The thresholds for artificial release should be confirmed in future comparisons of snow cover simulations with independent field data, such as records of signs of instability (e.g. Schweizer et al., 2021).

5.1.2. Avalanche observations

For evaluating our model, avalanche observations would ideally be separated by weak layer type or avalanche problem type and release times were accurate to the hour. However, crown profiles and direct visual observations are rare. Observers can often separate the trigger, but a limited number of observations hampers spatial coverage and even when using cameras for better coverage a correct estimate is limited by visibility (Helbig et al., 2015). We therefore used an avalanche catalogue obtained from seismic monitoring. Such data have high temporal resolution, which is particularly relevant for natural dry-snow avalanche release. The area covered by seismic monitoring systems (about 30 km^2) is much smaller than the typical size of an avalanche forecasting region ($>$ 200 km^2). Nevertheless, such systems can generally be used to identify the main avalanche periods (Heck et al., 2019), and in our case we combined data from two systems about 15 km apart.

The seismic avalanche data allowed us to calibrate snow instability indicators and evaluate simulated avalanche problems regarding natural release. We found the combination of the expected time to failure and the critical crack length provided a satisfying tradeoff in predicting avalanche days (POD $>$0.77 for SNOWPACK and Crocus) and detecting non-avalanche days (PON $>$ 0.66 for both models).

Comparing days with identified avalanche problems and days with natural release (Table 4) suggests that the model overestimates the number of avalanche days. On one hand, as our snow cover simulations can at best describe the situation around Weissfluhjoch, they are not necessarily indicative of the situation in the region around – which can be more variable than is reflected by the single, albeit representative measurement location. On the other hand, the area the sensor arrays cover may not be large enough to record enough natural avalanches to be indicative of the situation in the region. With perfect avalanche detection we could expect on the order of 1 or 10 natural avalanches per forecasting region when natural avalanche release is forecast as is typically the case with danger levels “considerable” or “high” (Schweizer et al., 2020). The seismic avalanche data had one day with more than 10 avalanches per day during the 2014–2015 season, whereas manual records at the Parsenn resort had 4 days with more than 10 avalanches only in January and February 2015.

5.1.3. Avalanche problems

Avalanche problem types were originally introduced to describe typical situations of avalanche danger (Atkins, 2005), which depends on snow cover and weather parameters. As snow cover models can predict weak and slab layers from weather input, we should be able to assess avalanche problem types from simulated slab and weak layer combinations. Our approach to assess avalanche problem types is much guided by snow layering, and weather data, such as 24-hour new snow, only alert for possible instabilities. Building on forecasting practices, which are weather-focused as snow cover information is usually sparse, decision trees have been created to assess avalanche problem types that characterize a prevailing avalanche situation (Horton et al., 2020).

With the use of snow cover models in avalanche forecasting it seems natural to develop an approach to assess avalanche problem types from snow cover model output. We laid out an algorithm that is partly based on expert knowledge, such as the characteristic active times of different weak layer types (Jamieson, 1995) and partly deterministic regarding snow instability modelling. Even though the combination of snow cover modelling and snow instability modelling was demonstrated for certain avalanche situations, temporarily (Reuter and Bellaire, 2018; Schweizer et al., 2016b) and spatially (Reuter et al., 2016), choosing the relevant weakness in the simulated snow cover has posed a challenge in the development process. In this context, two approaches were developed. (Mayer et al., 2021) used a random forest classification trained on a large data set of observed snow profiles (Schweizer et al., 2021) to detect weak layers. In this study we followed the weak layer after burial. Rather than following the weak layers from burial and assessing the stability during their lifetime, we could have simply chosen the weakest layer in the snowpack on a particular day. One could argue that the history of the weak layer and the potential slab are implicitly included in the simulated snow cover. Choosing avalanche problem types in a consistent way, however, proved difficult when just taking the weakest layer of the simulated snow profiles (Fig. 5). A snowfall, for instance, would change a persistent weak layer problem into a new snow problem, and natural or secondary release on the persistent weak layer problem could be missed. Interpretation of avalanche problems is straightforward when relevant weak layers are tracked.

Avalanche problem types have so far only been defined descriptively (EAWS, 2019; Statham et al., 2018), which makes the determination of avalanche problem types observer dependent. To overcome the challenge it holds for evaluating simulated avalanche problem types, we aggregated many seasons or cross-compared between SNOWPACK and Crocus simulations. Simulated avalanche problem types showed the same characteristic patterns that observations showed for two locations in Western Canada. Cross-comparing the model results at Weissfluhjoch demonstrated that with different snow cover models, similar avalanche problem type frequencies were obtained.

We found that avalanche problems can be assigned based on the weak layers identified in simulated stratigraphy. Using this approach in forecasting may facilitate a clearer interpretation at the practitioner's end. Currently, if a new snow problem is communicated it is often not clear whether or not a relevant persistent weak layer co-exists at the base of the new snow. The current algorithm may support forecasters to answer this difficult question. Moreover, our results suggest that usually more than one avalanche problem type is needed to characterize the avalanche situation which is in agreement with the analysis of Shandro and Haegeli (2018). Hence, avalanche forecasts should address the existing avalanche problems one by one.

5.1.4. Snow cover models

Running SNOWPACK and Crocus side by side for the same period allowed to assess model performance in view of snow instability. Both simulations showed agreement in the timing, the frequency of avalanche problem types and the trend to earlier wet-snow avalanches in the winters between 1999 and 2016 at Weissfluhjoch. Times when the models detected avalanche problems agreed qualitatively including the problem types (Fig. 7) for the season 2015–16 at Weissfluhjoch. The frequency of new snow and wind slab problems, the frequency of persistent weak layer problems and the frequency of wet-snow avalanche problems were similar in both models across 16 seasons (Fig. 8).

Differences between models can be related to the number of (aging-) persistent weak layers, to different snow transport indicators, and to differences during the snow melt period. Different snow cover modelling assumptions rules for instance for grain shape assessment can cause weak layers to disappear from the list of weak layers, as the weak layer assessment is different based on non-persistent and persistent grain shapes. The SNOWPACK flat field simulations include a simple drift index describing snow transport which assesses blowing snow based on snow availability and surface drag. We used the index to indicate wind slab problems. To flag wind slab problems in Crocus simulations, we implemented a similar routine with a constant friction velocity threshold. The different models led to inconsistent results between models across the seasons with generally less wind slab days in Crocus simulations and more days in SNOWPACK simulations. Moreover, the number of days with wind slab problems derived from SNOWPACK simulations increased over the period, whereas this number did not change much in Crocus simulations. The evaluation of wind slab problems is less reliable so far, and more work is needed to improve the assessment of wind slab problems. Including the additional load due to snow transport and weak layer formation during snow transport seem logical steps.

The date of the first wet-snow avalanche cycle in spring derived from the models were rather similar; differences occurred in the number of

potential wet-snow avalanche days which may be related to differences in how the two models treat liquid water. Melting and refreezing depends on simulated snow structure as well as on heat transport, where the models differ.

5.1.5. Snow climates

We detected avalanche problem types at locations in Western Canada, at Whistler and Rogers Pass, and in the Swiss Alps, at Weissfluhjoch. Based on numerical weather prediction data and SNOWPACK simulations we identified twice as many new snow than persistent weak layer problems in Whistler. At Rogers Pass avalanche problems were 5 times more often related to persistent weak layers than to new snow. In other words, the avalanche problem type new snow was twice as common in Whistler and persistent weak layers dominated at Rogers Pass – 6 times more common than in Whistler. The results confirm our expectation of an intermountain (Rogers Pass) and a maritime snow climate (Whistler). More importantly, these results provide us more confidence that the presented approach for avalanche problem type assessment works in different snow climates. Then, we should be able to predict possible shifts in avalanche problem characteristics when climates change.

The snow climate characteristics at Weissfluhjoch were in between the Canadian examples with persistent weak layer problems not as dominant as at Rogers Pass, and new snow problems not as frequent as in Whistler. Despite the short temporal extent of the data, both snow cover models simulated a trend to an earlier onset of the first wet-snow avalanches in spring (Fig. 8). The date of the first wet-snow avalanches at Weissfluhjoch shifted by about 10–14 days in 16 years and coincides with shorter winter seasons observed in the Alps over the past three decades (Matiu et al., 2021). With the presented approach longer time series can now be analyzed to study the climate impact on avalanche danger.

6. Conclusions

Based on snow cover model output, we developed a framework to assess avalanche problem types for natural release as well as for artificial triggering. The algorithm automatically identifies relevant weak layers and assesses their stability using current knowledge of avalanche formation. For a critical, well-documented avalanche situation we showed that weak layers observed in the field were detected and tracked in the simulations. We found agreement of the identified weak layers with field observations, and low values of calculated snow stability indicators that coincided with reported avalanches.

As there is no clear definition for snow instability regarding natural avalanche release, we explored combinations of snow instability indicators. Our results show that a combination of the expected time to failure and the critical crack length is best suited to describe failure initiation and crack propagation, respectively. Including a time derivative such as the expected time to failure allowed to account for the meteorological history and the dynamic evolution on the scale of hours, that are important for the likelihood of natural release. For artificial release we simulated the propensity to failure initiation and crack propagation as the current knowledge of avalanche release suggests and applied commonly used thresholds for snow instability, as data to determine the values are rare. We used the algorithm with two different snow cover models and applied the algorithm to three different locations and several winter seasons.

Assessing avalanche problem types in SNOWPACK and Crocus simulations yielded reasonable agreement with field data at Weissfluhjoch, Davos, Switzerland and Whistler and Rogers Pass, BC, Canada. Times and frequencies of avalanche problem types were similar and coincided with highly resolved natural avalanche activity data obtained with seismic monitoring, although some discrepancies remained – in particular related to snow transport.

We also show a time series of 17 winter seasons of avalanche problems between 1999 and 2016 at Weissfluhjoch, Davos. Simulated avalanche problem types were in 41 or 47% of the cases related to new snow or wind slabs, 37 or 31% of the cases related to persistent weak layers and in 22 and 21% related to wet-snow, for SNOWPACK and Crocus, respectively. The onset date of the wet-snow avalanche cycle in spring shifted at Weissfluhjoch by about 10–14 days during the 16-year period, consistent with other research that wet-snow avalanches release increasingly earlier in the last decades.

Simulated frequencies of avalanche problem types at Whistler and Rogers Pass in Western Canada agreed fairly well with the observed frequencies and showed the differences we expect between a maritime and an intermountain snow climate. Avalanche problems related to new snow were twice more common in Whistler than at Rogers Pass, which had six times more often avalanche problems related to persistent weak layers than Whistler.

The reasonable agreement with observations from different areas and different seasons provides confidence that the modelling approach can characterize avalanche danger with avalanche problem types – in situations with natural release or artificial triggering. The presented descriptions of avalanche problem types may be implemented in snow cover models to support avalanche forecasting in an operation. The method introduced here also holds potential for assessing past and future impacts of climate change on the characteristics of snow instability.

Data availability

Data presented in the article are available at www.envidat.ch: https://doi.org/10.16904/envidat.264

Author contributions

BR and SM acquired the funding for the project , based on a concept developed by BR. Data acquisition and curation: StM, LVG, PH and SH prepared the snow cover simulations. AvH prepared the seismic avalanche data. BR prepared the simulations of avalanche problem types. BR analyzed the simulated data, visulized the results and drafted the manuscript. The manuscript was reviewed and edited by all authors.

Financial support

BR was funded by the Swiss National Science Foundation (grant P400P2_186756 / 1). StM was funded by the WSL research program Climate Change Impacts on Alpine Mass Movements (CCAMM).

Declaration of Competing Interest

The authors declare that they have no conflict of interest.

Acknowledgements

We grateful to Karl Birkeland and an anonymous reviewer for their comments on the manuscript. We thank Sascha Bellaire, Christoph Mitterer and Jürg Schweizer for fruitful discussions on the topic.

References

Atkins, R., 2005. An avalanche characterization checklist for backcountry travel decisions. In: *Proceedings ISSW 2004. International Snow Science Workshop, Jackson Hole WY, U.S.A., 19-24 September 2004*, edited by K. Elder, pp. 462–468.

Baggi, S., Schweizer, J., 2009. Characteristics of wet snow avalanche activity: 20 years of observations from a high alpine valley (Dischma, Switzerland). Nat. Hazards 50 (1), 97–108.

Bair, E.H., 2013. Forecasting artificially-triggered avalanches in storm snow at a large ski area. Cold Reg. Sci. Technol. 85, 261–269. https://doi.org/10.1016/j.coldregions.2012.10.003.

Bartelt, P., Lehning, M., 2002. A physical SNOWPACK model for the Swiss avalanche warning; Part I: numerical model. Cold Reg. Sci. Technol. 35 (3), 123–145. https://doi.org/10.1016/S0165-232X(02)00074-5.

Bellaire, S., Jamieson, B., 2013. Forecasting the formation of critical snow layers using a coupled snow cover and weather model. Cold Reg. Sci. Technol. 94, 37–44. https://doi.org/10.1016/j.coldregions.2013.06.007.

Bellaire, S., van Herwijnen, A., Mitterer, C., Schweizer, J., 2017. On forecasting wet-snow avalanche activity using simulated snow cover data. Cold Reg. Sci. Technol. 144, 28–38. https://doi.org/10.1016/j.coldregions.2017.09.013.

Birkeland, K.W., 1998. Terminology and predominant processes associated with the formation of weak layers of near-surface faceted crystals in the mountain snowpack. Arct. Alp. Res. 30 (2), 193–199. https://doi.org/10.2307/1552134.

Birkeland, K.W., van Herwijnen, A., Reuter, B., Bergfeld, B., 2019. Temporal changes in the mechanical properties of snow related to crack propagation after loading. Cold Reg. Sci. Technol. 159, 142–152. https://doi.org/10.1016/j.coldregions.2018.11.007.

Breiman, L., Friedman, J.H., Olshen, R.A., Stone, C.J., 1998. Classification and Regression Trees, 368 pp. CRC Press, Boca Raton, U.S.A.

Brown, C.I., Jamieson, B., 2008. Shear strength and snowpack stability trends in non-persistant weak layers. In: Campbell, C., Conger, S., Haegeli, P. (Eds.), *Proceedings ISSW 2008, International Snow Science Workshop,* Whistler, Canada, *21–27 September 2008*, pp. 939–947.

Brun, E., Martin, E., Simon, V., Gendre, C., Coléou, C., 1989. An energy and mass model of snow cover suitable for operational avalanche forecasting. J. Glaciol. 35 (121), 333–342.

Brun, E., David, P., Sudul, M., Brunot, G., 1992. A numerical model to simulate snow-cover stratigraphy for operational avalanche forecasting. J. Glaciol. 38 (128), 13–22. https://doi.org/10.3189/S0022143000009552.

Calonne, N., Richter, B., Löwe, H., Cetti, C., ter Schure, J., van Herwijnen, A., Fierz, C., Jaggi, M., Schneebeli, M., 2020. The RHOSSA campaign: multi-resolution monitoring of the seasonal evolution of the structure and mechanical stability of an alpine snowpack. Cryosphere 14 (6), 1829–1848. https://doi.org/10.5194/tc-14-1829-2020.

Capelli, A., Reiweger, I., Lehmann, P., Schweizer, J., 2018. Fiber bundle model with time-dependent healing mechanisms to simulate progressive failure of snow. Phys. Rev. E 98 (2), 023002. https://doi.org/10.1103/PhysRevE.98.023002.

Castebrunet, H., Eckert, N., Giraud, G., Durand, Y., Morin, S., 2014. Projected changes of snow conditions and avalanche activity in a warming climate: the French Alps over the 2020-2050 and 2070-2100 periods. Cryosphere 8 (5), 1673–1697. https://doi.org/10.5194/tc-8-1673-2014.

Colbeck, S.C., 1988. On the micrometeorology of surface hoar growth on snow in mountain area. Bound.-Layer Meteorol. 44 (1–2), 1–12.

Colbeck, S.C., 1991. The layered character of snow covers. Rev. Geophys. 29 (1), 81–96.

Colbeck, S.C., 1998. The basic ideas behind snow metamorphism, *In: Snow as a physical, ecological and ecomomic factor*. In: Proceedings of the Symposium 60 years of Snow and Avalanche Research, *20–22 November 1996,* Davos, Switzerland, in press.

Conway, H., Wilbour, C., 1999. Evolution of snow slope stability during storms. Cold Reg. Sci. Technol. 30 (1–3), 67–77. https://doi.org/10.1016/S0165-232X(99)00009-9.

Conway, H., Breyfogle, S., Wilbour, C., 1989. Observations Relating to Wet Snow Stability, Paper Presented at Proceedings International Snow Science Workshop, Whistler, British Columbia, Canada, 12–15 October 1988, Canadian Avalanche Association, Vancouver BC, Canada, 1988/10/12–15.

de Quervain, M.R., 1966. Problems of Avalanche Research, Paper Presented at Symposium at Davos 1965 - Scientific Aspects of Snow and Ice Avalanches, IAHS Publication, 69, International Association of Hydrological Sciences, Wallingford, Oxfordshire, U.K.

Decharme, B., Boone, A., Delire, C., Noilhan, J., 2011. Local evaluation of the Interaction between Soil Biosphere Atmosphere soil multilayer diffusion scheme using four pedotransfer functions. J. Geophys. Res. Atmos. 116 (D20), D20126. https://doi.org/10.1029/2011jd016002.

Durand, Y., Giraud, G., Brun, E., Mérindol, L., Martin, E., 1999. A computer-based system simulating snowpack structures as a tool for regional avalanche forecasting. J. Glaciol. 45 (151), 469–484. https://doi.org/10.3189/S0022143000001337.

EAWS, 2019. Avalanche Problems, Edited, EAWS - European Avalanche Warning Services.

EAWS, 2021. Avalanche Danger Scale, Edited, EAWS - European Avalanche Warning Services.

Fawcett, T., 2006. An introduction to ROC analysis. Pattern Recogn. Lett. 27 (8), 861–874. https://doi.org/10.1016/j.patrec.2005.10.010.

Fierz, C., Armstrong, R.L., Durand, Y., Etchevers, P., Greene, E., McClung, D.M., Nishimura, K., Satyawali, P.K., Sokratov, S.A., 2009. The International Classification for Seasonal Snow on the Ground, 90 pp. UNESCO-IHP, Paris, France.

Gaume, J., Schweizer, J., van Herwijnen, A., Chambon, G., Reuter, B., Eckert, N., Naaim, M., 2014. Evaluation of slope stability with respect to snowpack spatial variability. J. Geophys. Res. 119 (9), 1783–1799. https://doi.org/10.1002/2014JF00319.

Gaume, J., van Herwijnen, A., Chambon, G., Wever, N., Schweizer, J., 2017. Snow fracture in relation to slab avalanche release: critical state for the onset of crack propagation. Cryosphere 11 (1), 217–228. https://doi.org/10.5194/tc-11-217-2017.

Gauthier, D., Brown, C., Jamieson, B., 2010. Modeling strength and stability in storm snow for slab avalanche forecasting. Cold Reg. Sci. Technol. 62 (2–3), 107–118. https://doi.org/10.1016/j.coldregions.2010.04.004.

Geldsetzer, T., Jamieson, J.B., 2001. Estimating dry snow density from grain form and hand hardness, paper presented at Proceedings ISSW 2000. In: International Snow Science Workshop, Big Sky, Montana, U.S.A., 1-6 October 2000, Montana State University, Bozeman MT, USA.

Giraud, G., Martin, E., Brun, E., Navarre, J.P., 2002. CrocusMepraPC software: a tool for local simulations of snow cover stratigraphy and avalanche risks, paper presented at Proceedings ISSW 2002. In: International Snow Science Workshop, Penticton BC, Canada, 29 September-4 October 2002.

Heck, M., Hobiger, M., van Herwijnen, A., Schweizer, J., Fäh, D., 2019. Localization of seismic events produced by avalanches using multiple signal classifications. Geophys. J. Int. 216 (1), 201–217. https://doi.org/10.1093/gji/ggy394.

Heierli, J., Gumbsch, P., Zaiser, M., 2008. Anticrack nucleation as triggering mechanism for snow slab avalanches. Science 321 (5886), 240–243. https://doi.org/10.1126/science.1153948.

Helbig, N., van Herwijnen, A., Jonas, T., 2015. Forecasting wet-snow avalanche probability in mountainous terrain. Cold Reg. Sci. Technol. 120, 219–226. https://doi.org/10.1016/j.coldregions.2015.07.001.

Horton, S., Nowak, S., Haegeli, P., 2019. Enhancing the operational value of snowpack models with visualization design principles. Nat. Hazards Earth Syst. Sci. 20 (6), 1557–1572. https://doi.org/10.5194/nhess-20-1557-2020.

Horton, S., Towell, M., Haegeli, P., 2020. Examining the operational use of avalanche problems with decision trees and model-generated weather and snowpack variables. Nat. Hazards Earth Syst. Sci. 20 (12), 3551–3576. https://doi.org/10.5194/nhess-20-3551-2020.

Jamieson, J.B., 1995. Avalanche Prediction for Persistent Snow Slabs, Ph.D. Thesis, 258 Pp. University of Calgary, Calgary AB, Canada.

Jamieson, J.B., 1999. The compression test - after 25 years. Avalanche Rev. 18 (1), 10–12.

Jamieson, J.B., Johnston, C.D., 1995. Monitoring a shear frame stability index and skier-triggered slab avalanches involving persistent snowpack weaknesses, paper presented at Proceedings ISSW 1994. In: International Snow Science Workshop, Snowbird, Utah, U.S.A., 30 October-3 November 1994, ISSW 1994 Organizing Committee, Snowbird UT, USA.

Jamieson, J.B., Zeidler, A., Brown, C., 2007. Explanation and limitations of study plot stability indices for forecasting dry snow slab avalanches in surrounding terrain. Cold Reg. Sci. Technol. 50 (1–3), 23–34. https://doi.org/10.1016/j.coldregions.2007.02.010.

LaChapelle, E.R., 1966. Avalanche forecasting - a modern synthesis. IAHS Publ. 69, 350–356.

Lafaysse, M., Morin, S., Coléou, C., Vernay, M., Serça, D., Besson, F., Willemet, J.M., Giraud, G., Durand, Y., 2013. Towards a new chain of models for avalanche hazard forecasting in French mountain ranges, including low altitude mountains, paper presented at Proceedings ISSW 2013. In: International Snow Science Workshop, Grenoble, France, 7–11 October 2013, ANENA, IRSTEA, Météo-France, Grenoble, France.

Lafaysse, M., Cluzet, B., Dumont, M., Lejeune, Y., Vionnet, V., Morin, S., 2017. A multiphysical ensemble system of numerical snow modelling. Cryosphere 11 (3), 1173–1198. https://doi.org/10.5194/tc-11-1173-2017.

Lehning, M., Fierz, C., 2008. Assessment of snow transport in avalanche terrain. Cold Reg. Sci. Technol. 51 (2–3), 240–252. https://doi.org/10.1016/j.coldregions.2007.05.012.

Lehning, M., Bartelt, P., Brown, R.L., Fierz, C., 2002a. A physical SNOWPACK model for the Swiss avalanche warning; Part III: meteorological forcing, thin layer formation and evaluation. Cold Reg. Sci. Technol. 35 (3), 169–184. https://doi.org/10.1016/S0165-232X(02)00072-1.

Lehning, M., Bartelt, P., Brown, R.L., Fierz, C., Satyawali, P.K., 2002b. A physical SNOWPACK model for the Swiss avalanche warning; Part II. Snow microstructure. Cold Reg. Sci. Technol. 35 (3), 147–167. https://doi.org/10.1016/S0165-232X(02)00073-3.

Lehning, M., Fierz, C., Brown, R.L., Jamieson, J.B., 2004. Modeling instability for the snow cover model SNOWPACK. Ann. Glaciol. 38, 331–338. https://doi.org/10.3189/172756404781815220.

Li, L., Pomeroy, J.W., 1997. Estimates of threshold wind speeds for snow transport using meteorological data. J. Appl. Meteorol. 36 (3), 205–213. https://doi.org/10.1175/1520-0450(1997)036<0205:Eotwsf>2.0.Co;2.

Marchetti, E., Ripepe, M., Ulivieri, G., Kogelnig, A., 2015. Infrasound array criteria for automatic detection and front velocity estimation of snow avalanches: towards a real-time early-warning system. Nat. Hazards Earth Syst. Sci. 15 (11), 2545–2555. https://doi.org/10.5194/nhess-15-2545-2015.

Marchetti, E., van Herwijnen, A., Christen, M., Silengo, M.C., Barfucci, G., 2020. Seismo-acoustic energy partitioning of a powder snow avalanche. Earth Surf. Dyn. 8 (2), 399–411. https://doi.org/10.5194/esurf-8-399-2020.

Marienthal, A., Hendrikx, J., Birkeland, K., Irvine, K.M., 2015. Meteorological variables to aid forecasting deep slab avalanches on persistent weak layers. Cold Reg. Sci. Technol. 120, 227–236. https://doi.org/10.1016/j.coldregions.2015.08.007.

Marshall, H.-P., Johnson, J.B., 2009. Accurate inversion of high-resolution snow penetrometer signals for microstructural and micromechanical properties. J. Geophys. Res. 114 (F4), F04016. https://doi.org/10.1029/2009jf001269.

Matiu, M., et al., 2021. Observed snow depth trends in the European Alps: 1971 to 2019. Cryosphere 15 (3), 1343–1382. https://doi.org/10.5194/tc-15-1343-2021.

Mayer, S., van Herwijnen, A., Ulivieri, G., Schweizer, J., 2020. Evaluating the performance of an operational infrasound avalanche detection system at three locations in the Swiss Alps during two winter seasons. Cold Reg. Sci. Technol. 173, 102962 https://doi.org/10.1016/j.coldregions.2019.102962.

Mayer, S., van Herwijnen, A., Schweizer, J., 2021. A random forest model to assess snow instability from simulated snow stratigraphy. In: *EGU General Assembly 2021, online*, EGU21-12259. https://doi.org/10.5194/egusphere-egu21-12259.

McClung, D.M., 1981. Fracture mechanical models of dry slab avalanche release. J. Geophys. Res. 86 (B11), 10783–10790. https://doi.org/10.1029/JB086iB11p10783.

McClung, D.M., Schweizer, J., 1999. Skier triggering, snow temperatures and the stability index for dry slab avalanche initiation. J. Glaciol. 45 (150), 190–200.

Ménard, C.B., et al., 2019. Meteorological and evaluation datasets for snow modelling at 10 reference sites: description of in situ and bias-corrected reanalysis data. Earth Syst. Sci. Data 11 (2), 865–880. https://doi.org/10.5194/essd-11-865-2019.
Milbrandt, J.A., Bélair, S., Faucher, M., Vallée, M., Carrera, M.L., Glazer, A., 2016. The Pan-Canadian high resolution (2.5 km) deterministic prediction system. Weather Forecast. 31 (6), 1791–1816. https://doi.org/10.1175/waf-d-16-0035.1.
Mitterer, C., Schweizer, J., 2013. Analysis of the snow-atmosphere energy balance during wet-snow instabilities and implications for avalanche prediction. Cryosphere 7 (1), 205–216. https://doi.org/10.5194/tc-7-205-2013.
Mitterer, C., Techel, F., Fierz, C., Schweizer, J., 2013. An operational supporting tool for assessing wet-snow avalanche danger, paper presented at Proceedings ISSW 2013. In: International Snow Science Workshop, Grenoble, France, 7–11 October 2013, ANENA, IRSTEA, Météo-France, Grenoble, France.
Mitterer, C., Heilig, A., Schmid, L., van Herwijnen, A., Eisen, O., Schweizer, J., 2016. Comparison of measured and modelled snow cover liquid water content to improve local wet-snow avalanche prediction, paper presented at Proceedings ISSW 2016. In: International Snow Science Workshop, Breckenridge CO, U.S.A., 3–7 October 2016.
Mock, C.J., Birkeland, K.W., 2000. Snow avalanche climatology of the western United States mountain ranges. Bull. Am. Meteorol. Soc. 81 (10), 2367–2392.
Monti, F., Schweizer, J., Fierz, C., 2014. Hardness estimation and weak layer detection in simulated snow stratigraphy. Cold Reg. Sci. Technol. 103, 82–90.
Monti, F., Gaume, J., van Herwijnen, A., Schweizer, J., 2016. Snow instability evaluation: calculating the skier-induced stress in a multi-layered snowpack. Nat. Hazards Earth Syst. Sci. 16 (3), 775–788. https://doi.org/10.5194/nhess-16-775-2016.
Morin, S., et al., 2020. Application of physical snowpack models in support of operational avalanche hazard forecasting: a status report on current implementations and prospects for the future. Cold Reg. Sci. Technol. 170, 102910 https://doi.org/10.1016/j.coldregions.2019.102910.
Nadreau, J.P., Michel, B., 1986. Yield and failure envelope for ice under multiaxial compressive stresses. Cold Reg. Sci. Technol. 13 (1), 75–82.
Nishimura, K., Baba, E., Hirashima, H., Lehning, M., 2005. Application of the snow cover model SNOWPACK to snow avalanche warning in Niseko, Japan. Cold Reg. Sci. Technol. 43 (1–2), 62–70. https://doi.org/10.1016/j.coldregions.2005.05.007.
Perla, R., LaChapelle, E.R., 1970. A theory of snow slab failure. J. Geophys. Res. 75 (36), 7619–7627.
Reuter, B., Bellaire, S., 2018. On combining snow cover and snow instability modelling, paper presented at Proceedings ISSW 2018. In: International Snow Science Workshop, Innsbruck, Austria, 7-12 October 2018.
Reuter, B., Schweizer, J., 2018. Describing snow instability by failure initiation, crack propagation, and slab tensile support. Geophys. Res. Lett. 45 (14), 7019–7027. https://doi.org/10.1029/2018GL078069.
Reuter, B., Schweizer, J., van Herwijnen, A., 2015a. A process-based approach to estimate point snow instability. Cryosphere 9, 837–847. https://doi.org/10.5194/tc-9-837-2015.
Reuter, B., van Herwijnen, A., Veitinger, J., Schweizer, J., 2015b. Relating simple drivers to snow instability. Cold Reg. Sci. Technol. 120, 168–178. https://doi.org/10.1016/j.coldregions.2015.06.016.
Reuter, B., Richter, B., Schweizer, J., 2016. Snow instability patterns at the scale of a small basin. J. Geophys. Res. Earth Surf. 121 (2), 257–282. https://doi.org/10.1002/2015JF003700.
Richter, B., Schweizer, J., Rotach, M.W., van Herwijnen, A., 2019. Validating modeled critical crack length for crack propagation in the snow cover model SNOWPACK. Cryosphere 13 (12), 3353–3366. https://doi.org/10.5194/tc-13-3353-2019.
Richter, B., van Herwijnen, A., Rotach, M., Schweizer, J., 2020. Sensitivity of modeled snow stability data to meteorological input uncertainty. Nat. Hazards Earth Syst. Sci. 20 (11), 2873–2888. https://doi.org/10.5194/nhess-20-2873-2020.
Roch, A., 1966. Les Variations de la résistance de la Neige, Paper Presented at Symposium at Davos 1965 - Scientific Aspects of Snow and Ice Avalanches, IAHS Publication, 69. International Association of Hydrological Sciences, Wallingford, Oxfordshire, U.K.
Schweizer, J., Jamieson, J.B., 2003. Snowpack properties for snow profile analysis. Cold Reg. Sci. Technol. 37 (3), 233–241. https://doi.org/10.1016/S0165-232X(03)00067-3.
Schweizer, J., Jamieson, J.B., 2010. Snowpack tests for assessing snow-slope instability. Ann. Glaciol. 51 (54), 187–194. https://doi.org/10.3189/172756410791386652.
Schweizer, J., Bellaire, S., Fierz, C., Lehning, M., Pielmeier, C., 2006. Evaluating and improving the stability predictions of the snow cover model SNOWPACK. Cold Reg. Sci. Technol. 46 (1), 52–59. https://doi.org/10.1016/j.coldregions.2006.05.007.
Schweizer, J., McCammon, I., Jamieson, J.B., 2008. Snowpack observations and fracture concepts for skier-triggering of dry-snow slab avalanches. Cold Reg. Sci. Technol. 51 (2–3), 112–121. https://doi.org/10.1016/j.coldregions.2007.04.019.
Schweizer, J., Mitterer, C., Stoffel, L., 2009. On forecasting large and infrequent snow avalanches. Cold Reg. Sci. Technol. 59 (2–3), 234–241. https://doi.org/10.1016/j.coldregions.2009.01.006.
Schweizer, J., van Herwijnen, A., Reuter, B., 2011. Measurements of weak layer fracture energy. Cold Reg. Sci. Technol. 69 (2–3), 139–144. https://doi.org/10.1016/j.coldregions.2011.06.004.
Schweizer, J., Reuter, B., van Herwijnen, A., Gaume, J., 2016a. Avalanche release 101, paper presented at proceedings ISSW 2016. In: International Snow Science Workshop, Breckenridge CO, U.S.A., 3-7 October 2016.
Schweizer, J., Reuter, B., van Herwijnen, A., Richter, B., Gaume, J., 2016b. Temporal evolution of crack propagation propensity in snow in relation to slab and weak layer properties. Cryosphere 10 (6), 2637–2653. https://doi.org/10.5194/tc-10-2637-2016.
Schweizer, J., Mitterer, C., Techel, F., Stoffel, A., Reuter, B., 2020. On the relation between avalanche occurrence and avalanche danger level. Cryosphere 14 (2), 737–750. https://doi.org/10.5194/tc-14-737-2020.
Schweizer, J., Mitterer, C., Reuter, B., Techel, F., 2021. Avalanche danger level characteristics from field observations of snow instability. Cryosphere 15 (7), 3293–3315. https://doi.org/10.5194/tc-15-3293-2021.
Shandro, B., Haegeli, P., 2018. Characterizing the nature and variability of avalanche hazard in western Canada. Nat. Hazards Earth Syst. Sci. 18 (4), 1141–1158. https://doi.org/10.5194/nhess-18-1141-2018.
Simenhois, R., Birkeland, K.W., 2009. The extended column test: test effectiveness, spatial variability, and comparison with the propagation saw test. Cold Reg. Sci. Technol. 59 (2–3), 210–216. https://doi.org/10.1016/j.coldregions.2009.04.001.
SLF, 2016. *SLF-Beobachterhandbuch*, WSL-Institut für Schnee- und Lawinenforschung SLF, 7260 Davos; Eidg. Forschungsanstalt für Wald, Schnee und Landschaft WSL, CH-8903 Birmensdorf, Davos, Switzerland.
Statham, G., Haegeli, P., Greene, E., Birkeland, K., Israelson, C., Tremper, B., Stethem, C., McMahon, B., White, B., Kelly, J., 2018. A conceptual model of avalanche hazard. Nat. Hazards 90 (2), 663–691. https://doi.org/10.1007/s11069-017-3070-5.
Stoffel, A., Meister, R., Schweizer, J., 1998. Spatial characteristics of avalanche activity in an alpine valley - a GIS approach. Ann. Glaciol. 26, 329–336. https://doi.org/10.3189/1998AoG26-1-329-336.
Techel, F., Müller, K., Schweizer, J., 2020. On the importance of snowpack stability, the frequency distribution of snowpack stability, and avalanche size in assessing the avalanche danger level. Cryosphere 14 (10), 3503–3521. https://doi.org/10.5194/tc-14-3503-2020.
Ulivieri, G., Marchetti, E., Ripepe, M., Chiambretti, I., Rosa, G.D., Segor, V., 2011. Monitoring snow avalanches in Northwestern Italian Alps using an infrasound array. Cold Reg. Sci. Technol. 69 (2–3), 177–183. https://doi.org/10.1016/j.coldregions.2011.09.006.
van Herwijnen, A., Schweizer, J., 2011. Seismic sensor array for monitoring an avalanche start zone: design, deployment and preliminary results. J. Glaciol. 57 (202), 267–276. https://doi.org/10.3189/002214311796405933.
van Herwijnen, A., Gaume, J., Bair, E.H., Reuter, B., Birkeland, K.W., Schweizer, J., 2016. Estimating the effective elastic modulus and specific fracture energy of snowpack layers from field experiments. J. Glaciol. 62 (236), 997–1007. https://doi.org/10.1017/jog.2016.90.
Vernay, M., Lafaysse, M., Mérindol, L., Giraud, G., Morin, S., 2015. Ensemble forecasting of snowpack conditions and avalanche hazard. Cold Reg. Sci. Technol. 120, 251–262. https://doi.org/10.1016/j.coldregions.2015.04.010.
Vionnet, V., Brun, E., Morin, S., Boone, A., Faroux, S., Le Moigne, P., Martin, E., Willemet, J.M., 2012. The detailed snowpack scheme Crocus and its implementation in SURFEX v7.2. Geosci. Model Dev. 5 (3), 773–791. https://doi.org/10.5194/gmd-5-773-2012.
Wever, N., 2017. Weissfluhjoch Dataset for ESM-SnowMIP, in *EnviDat*, edited, WSL Institute for Snow and Avalanche Research SLF. https://doi.org/10.16904/16.
Wever, N., Vera Valero, C., Fierz, C., 2016. Assessing wet snow avalanche activity using detailed physics based snowpack simulations. Geophys. Res. Lett. 43, 5732–5740. https://doi.org/10.1002/2016GL068428.
Wilks, D.S., 2011. Statistical Methods in the Atmospheric Sciences, 3rd ed., 467 pp. Academic Press, San Diego CA, U.S.A.